AD_____

Award Number: W81XWH-10-1-0864

TITLE: A Clinically Realistic Large Animal Model of Intra-Articular Fracture

PRINCIPAL INVESTIGATOR: Jessica E. Goetz, Ph.D.

CONTRACTING ORGANIZATION: The University of Iowa
Iowa City, IA 52242

REPORT DATE: October 2013

TYPE OF REPORT: Annual

PREPARED FOR: U.S. Army Medical Research and Materiel Command
Fort Detrick, Maryland 21702-5012

REPORT DOCUMENTATION PAGE

Form Approved
OMB No. 0704-0188

1. REPORT DATE	**2. REPORT TYPE**	**3. DATES COVERED**
October 2013	Annual	15 September 2012 – 14 September 2013

4. TITLE AND SUBTITLE
A Clinically Realistic Large Animal Model of Intra-Articular Fracture

5a. CONTRACT NUMBER

5b. GRANT NUMBER
W81XWH-10-1-0864

5c. PROGRAM ELEMENT NUMBER

6. AUTHOR(S)
Jessica E. Goetz, Ph.D.

E-Mail: jessica-goetz@uiowa.edu

5d. PROJECT NUMBER

5e. TASK NUMBER

5f. WORK UNIT NUMBER

7. PERFORMING ORGANIZATION NAME(S) AND ADDRESS(ES)

University of Iowa
Iowa City, Iowa 52242-1100

8. PERFORMING ORGANIZATION REPORT NUMBER

9. SPONSORING / MONITORING AGENCY NAME(S) AND ADDRESS(ES)
U.S. Army Medical Research and Materiel Command
Fort Detrick, Maryland 21702-5012

10. SPONSOR/MONITOR'S ACRONYM(S)

11. SPONSOR/MONITOR'S REPORT NUMBER(S)

12. DISTRIBUTION / AVAILABILITY STATEMENT
Approved for Public Release; Distribution Unlimited

13. SUPPLEMENTARY NOTES

14. ABSTRACT

The primary objective of this project is to develop a novel large animal survival model of intra-articular fracture (IAF) in which all major pathophysiological attributes corresponding to human injuries are realistically replicated, and in which post-traumatic osteoarthritis (PTOA) predictably develops. Building upon the work and protocols developed during the first two project years, substantial progress was made during this third project year (PY3), to establish the natural history of intra-articular fracture in the porcine model. All long-term survival experiments were completed, and the healing response, animal activity data, and inflammation history data have been analyzed. The fracture and repair protocol results in well-healed joints which the animal begins to load normally 2-4 weeks after surgical insult, and the inflammatory response is similar to that seen in injured human joints. During the upcoming PY4, the final histological analysis of these long-term experiments will be conducted, and the short-term survival study investigating the effects of therapeutic treatment which was initiated during PY3 will be completed.

15. SUBJECT TERMS
post-traumatic osteoarthritis, joint injuries, intra-articular fracture, survival animal model, cartilage degeneration

16. SECURITY CLASSIFICATION OF:			**17. LIMITATION OF ABSTRACT**	**18. NUMBER OF PAGES**	**19a. NAME OF RESPONSIBLE PERSON**
a. REPORT	**b. ABSTRACT**	**c. THIS PAGE**			USAMRMC
U	U	U	UU	40	**19b. TELEPHONE NUMBER** *(include area code)*

Table of Contents

Appendices (23 pages):

1. Diestelmeier BW, Rudert MJ, Tochigi Y, Baer TE, Fredericks DC, Brown TD. *An instrumented pendulum system for measuring energy absorption during fracture insult to large animal joints in vivo.* J Biomech Eng. (In Press).
2. Roberts N, Martin JA, Fredericks DC, Tochigi Y, Goetz JE. Fluctuation of synovial fluid inflammatory cytokine concentrations in an animal model of intra-articular fracture. 2014 Annual Meeting of the Orthopaedic Research Society, March 15-18, 2014, New Orleans, LA. (submitted)
3. Coleman MC, Fredericks DC, Martin JA, Goetz JE. *Intraarticular administration of n-acetyl cysteine and glycyrrhizin alleviates acute oxidative stress following intraarticular fracture.* 2014 Annual Meeting of the Orthopaedic Research Society, March 15-18, 2014, New Orleans, LA. (submitted)

1. INTRODUCTION

The primary objective of this project is to develop a novel large animal survival model of intra-articular fracture (IAF) in which all major pathophysiological attributes of corresponding human clinical injuries are realistically replicated, and in which post-traumatic osteoarthritis (OA) predictably develops. Specifically, work has been proposed to thoroughly validate the fracture insult technique/system developed for introducing pathophysiologically realistic IAFs in the porcine hock *in vivo* (Aim 1), to establish post-insult management methodology (Aim 2), and to validate the capability of the animal model as a research tool for piloting new treatment methods (Aim 3). At the conclusion of the project, we expect to have established a definitive methodology to create a clinically realistic large animal survival model of IAF, and we expect to have demonstrated the value of the animal model as a powerful new translational research tool. This animal model will facilitate translational research of orthopaedic treatment for IAFs, specifically by providing opportunities to test efficacy and safety of new treatment strategies prior to clinical trial, advancing orthopaedic treatment to mitigate the risk of OA following IAFs.

2. BODY

2.1 Administrative & Personnel Changes

During Project Year 3, Dr. Yuki Tochigi, the principal investigator leading this project left the University of Iowa to return to his family in Japan. Dr. Jessica Goetz assumed the role of Principal Investigator on this project effective 8/1/2013. As a result of Dr. Tochigi's departure, several project activities were delayed, and a one-year extension of the project was granted to complete the activities outlined in the SOW.

2.2 Summary of Previous Work & Completed Task 1

As reported in the previous progress reports, the work in PY1 and PY2 has resulted in a definitive impaction technique for introducing a consistent intra-articular fracture in the porcine hock *in vivo* (Task 1). A suitable fracture fixation methodology was also finalized which provided sufficient stabilization of the injury to facilitate fracture healing and allowed the animal to ambulate reasonably normally within a short period of time after injury.

2.2.a Fracture Insult Methodology & Post-Insult Management

Under general anesthesia, each animal is subjected to a fracture insult of the left hock using a purpose-designed "offset" impaction technique (Figure 1).[1,2] First, the distal impact "tripod" is anchored to the talus through the calcaneus using three cortical pins (Figure 2). This device facilitates direct delivery of a fracture force pulse through the experimental joint without energy loss associated with soft tissue absorption or compression of the subtalar joint. Next, a transverse stress-rising saw cut is placed across the anterior cortex of the tibia (leaving a 5 mm-thick zone of juxta-articular bone intact) to guide the location and orientation of fracture line. The distal tibial shaft of the experimental leg is secured to a custom pendulum-based impaction apparatus in a posteriorly tilted "offset" position (Figure 1). The fracturing force pulse is then delivered using a 5.8 kg pendulum mass released from a user-controlled height of 79 cm, which generate 45 joules of kinetic energy. The energy absorbed during the impaction insult (causing the fracture) is determined by measuring the difference between energy delivered (the pendulum's kinetic energy immediately before impaction) and energy passed through the specimen (energy transmitted to the sled-spring instrument to which the tibia holder is mounted).[1]

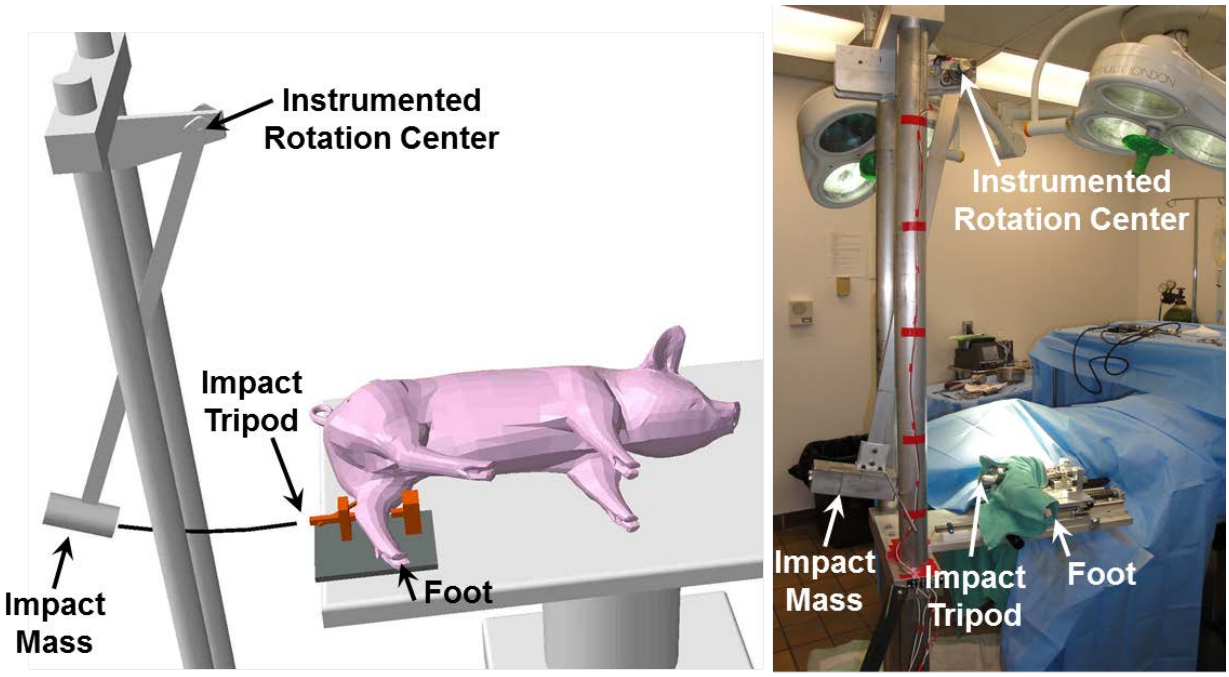

Figure 1. Schematic of animal orientation during surgical impact (left) illustrating the position of the animal beneath the drape during surgery (right).

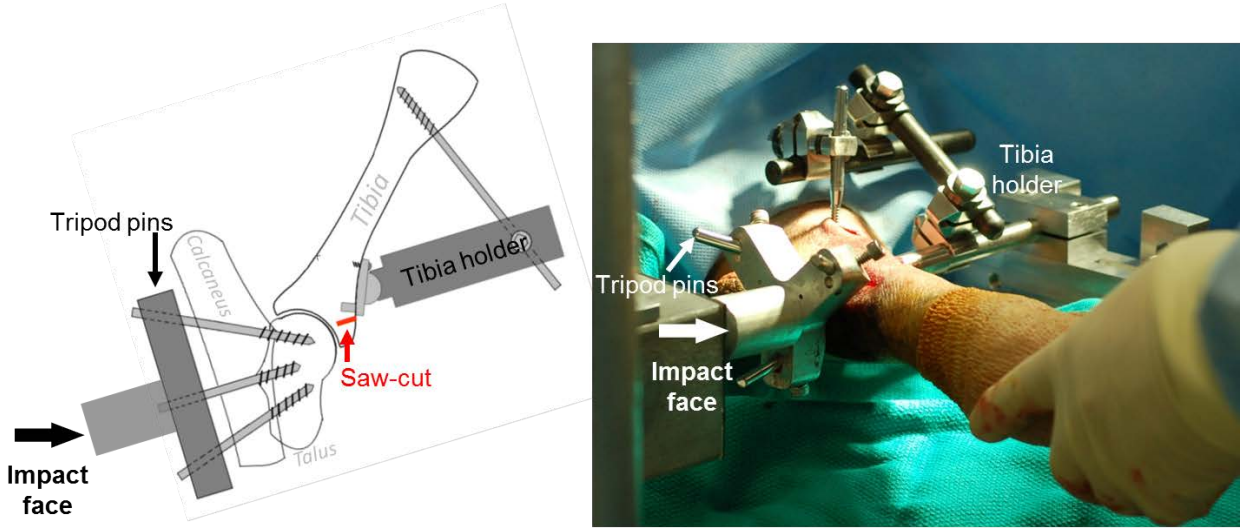

Figure 2. Schematic of the tripod impaction device applied to the bones of the pig hock (left) and intra-operative application of the tripod impaction device (right). The impact mass of the pendulum swings down and contacts the impact face of the tripod, which passes the energy through the calcaneus to the talus via the tripod pins. The talus is driven into the anterior portion of the tibia causing an intra-articular fracture extending through the saw cut.

Immediately following the impact insult, the tripod and pendulum attachment hardware devices are removed and the experimental fractures are surgically stabilized. The internal fixation technique utilized (Figure 3) is very consistent with “standard-of-care” techniques for

human clinical intraarticular fractures. The primary fixation implant is a clover-shaped locking plate designed for canine proximal tibial osteotomy (SYNTHES® Vet 2.7 mm TPLO plate, Synthes GmbH, Solothurn, Switzerland). This plate is placed on the anterior aspect of the distal tibial shaft using three bi-cortical screws, so as to provide a "buttress" effect for the anterior malleolar fragment. Through the central hole of the clover-shaped head, a distal locking screw is placed for fragment stabilization. To provide additional rotational stability, a combination of additional screws through the cloverleaf and/or an antero-medial screw outside of the clover plate may be added at the discretion of the surgeon. In experiments where a 2-mm step-off was introduced to replicate residual joint incongruity following mal-reduced fracture fixation, an extra small T-plate is utilized to provide additional stability. However this extra hardware is not needed for performing an anatomic repair. During the first week after surgery, the fractured and surgically repaired limb is provided supplemental external stabilization with a fiberglass cast. Post-operatively, the animals are permitted unlimited activity under pen confinement.

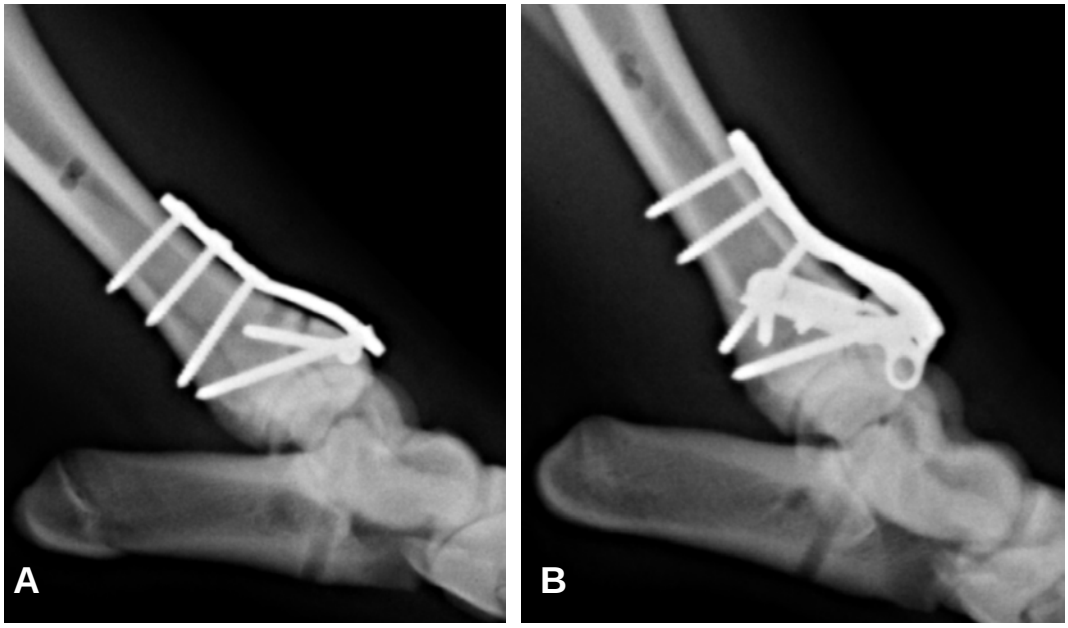

Figure 3. Representative cases of internal fixation techniques for anatomical reduction cases (A) and step-off reduction cases (B).

2.2.b Radiographic Bone Healing

Fracture fixation stability and bone healing were monitored radiographically at 3 days and at 1, 2, 4, 8, and 12 weeks after index surgery. At the time of the previous progress report, the first three series of animals had been sacrificed, and radiographic union was seen in all 14 animals at this 12 week time point. Presently, fixation of all animals have been completed, and stable fracture healing was achieved in all 18 animals at 12 weeks. The only complication related to healing was in experimental animal #3, in which a delayed union was apparent on radiograph, specifically widening of the fracture gap (from week 2), which in turn resulted in decreasing density of the anterior malleolar fragment. However, when this experimental joint was dissected 12 weeks post-surgery, stable bone healing was apparent upon manual inspection. While there were three fracture dislocations in the early two series of experiments, there were no fixation or healing failures in the third and fourth experimental series, leading us to conclude that those early failures can be attributed to technique development.

2.3 PY3 Progress on Establishment of Analysis Methods (Task 2) & Establishing the Natural History of Injury (Task 3)

The surgery and sacrifice of the animals proposed to address Specific Aims 1 & 2 of this project have been completed. The survival period of the final group of animals ended in February 2013, which has allowed for the analysis of the majority of the outcome measures that will be used for establishing the natural history of this porcine model. The details of the 18 animals that comprise this group are shown in Table 1.

Table 1. Details of the animals in Specific Aims 1 & 2. The number of impacts used to create the fracture and any complications are listed. Four animals had to be sacrificed before the full 12-week survival time due to complications indicated below.

	Test	Reduction	Impact Count	Complication	Action/Outcome
May 2011 Series	1	Anatomical	4	Hip dislocation	Early Sacrifice (4 days post-op)
	2	Anatomical	1		
	3	Anatomical	1	Delayed union	
	4	Step-Off	2		
April 2012 Series	5	Anatomical	1	Screw exposure	
	6	Anatomical	2		
	7	Step-Off	1	Fracture dislocation	Early Sacrifice (2 weeks post-op)
	8	Anatomical	1		
	9	Step-Off	1	Spontaneous reduction	
	10	Anatomical	2		
	11	Step-Off	1	Fracture dislocation	Early Sacrifice (1 week post-op)
July 2012 Series	12	Step-Off	1		
	13	Anatomical	1		
	14	Step-Off	1		
	15	Step-Off	1		
	16	Step-Off	1		
	17	Anatomical	1	Screw exposure	
November 2012 Series	18	Step-Off	1	Infection + Talus Fracture	Early Sacrifice (8 weeks post-op)
	19	Anatomical	1		
	20	Step-Off	1		
	21	Anatomical	1		
	22	Anatomical	1		

2.3.a Fracture Morphology & Morphological Residuals

2.3.a.1 Radiographic Evaluation: Radiographs were primarily used in this work to evaluate suitable progression of fracture healing. Fracture fragment size and shape were evaluated qualitatively and found to be a single fragment in the anterior portion of the distal tibia for all eighteen animals. The fragment was seen to remain in its original immediate post-operative location (Figure 4), indicating the surgical fixation was adequate to maintain the initial reduction (anatomic or step-off) until bony union was achieved.

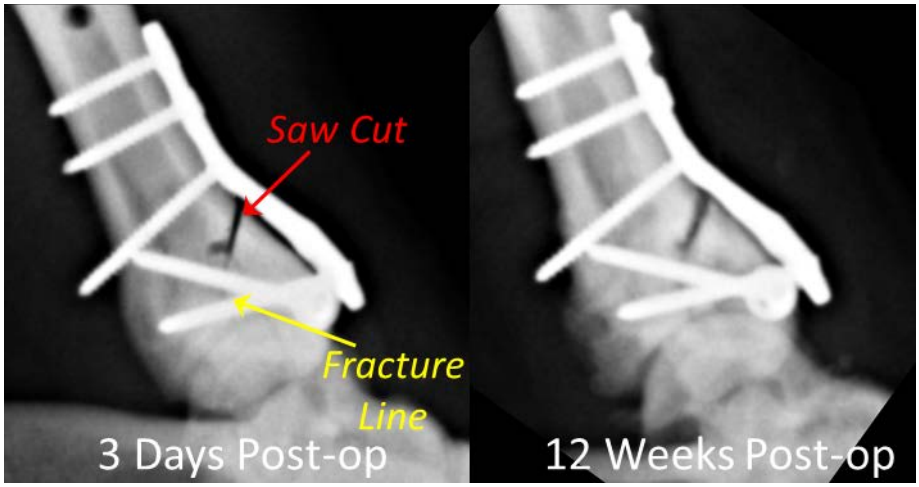

Figure 4. Radiographs of a fracture created in Series 4. The saw cut is clear and the fracture line closed early post-operatively (right). At the time of sacrifice, the fragment has healed in the proper location, with an indistinct fracture line and a less defined saw cut visible.

2.3.a.2 Evaluation of Joint Surface Incongruity: For every experimental joint, CT scans (0.3mm x 0.3mm x 1mm voxels) were acquired prior to fracture (baseline) and 12 weeks after index surgery. The outer cortex of the distal tibia was segmented using OsiriX software (Pixmeo, Geneva, Switzerland) for limbs scanned with the fixation hardware in place, or using a custom segmentation program developed in Matlab (The Mathworks, Natick, MA) for limbs without hardware. All segmentations were smoothed into a continuous 3D surface using Geomagic Studio (Geomagic, Morrisville, NC, USA). Surfaces generated from post-surgery CT images were registered to their respective pre-surgery surfaces using an iterative closest-point technique in Geomagic Studio. The technique aligned the tibial shaft and the medial to posterior epiphyseal bone of the fracture case to the intact surface while temporarily disregarding deviations resulting from the fracture.

The maximum and the average distance between the registered surfaces perpendicular to the intact joint surface is calculated as a first measure of changes in joint surface morphology (Figure 5). The percentage of the articular surface

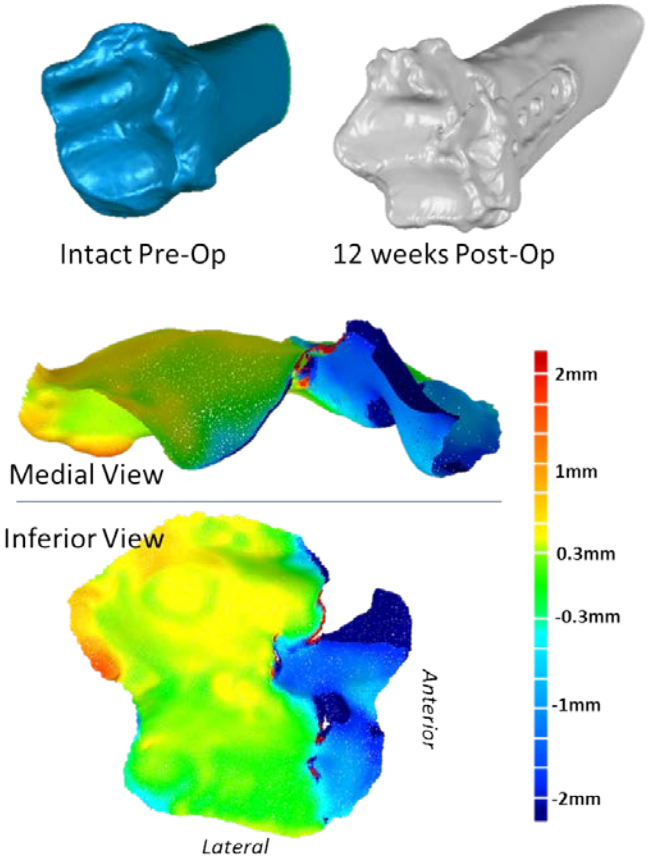

Figure 5. Illustration of methods for CT-based evaluation of articular surface incongruity. The intact pre-op surface (top left) was used as a template, and the 12 week post op surface (top right) was aligned to that template. The articular surface of both joints (pre- and post-op) was extracted (bottom) and the depth of the operative surface was quantified as distance from the normal joint surface.

depressed more than 1, 2, 3, 4, and 5 millimeters was also quantified to determine the extent to which the entire joint surface was affected. As expected, animals that were intentionally reduced with a 2mm step-off had a greater amount of the total joint surface that was more depressed from the normal surface at the time of sacrifice (Figure 6). However, the maximum depth of depression seen in animals with an intentional step-off was not appreciably different from animals with an anatomic fracture reduction. This is likely a result of a small area of focal surface depression or non-mineralized repair tissue in the fracture line not demonstrating CT signal that was intense enough to be identified as bone.

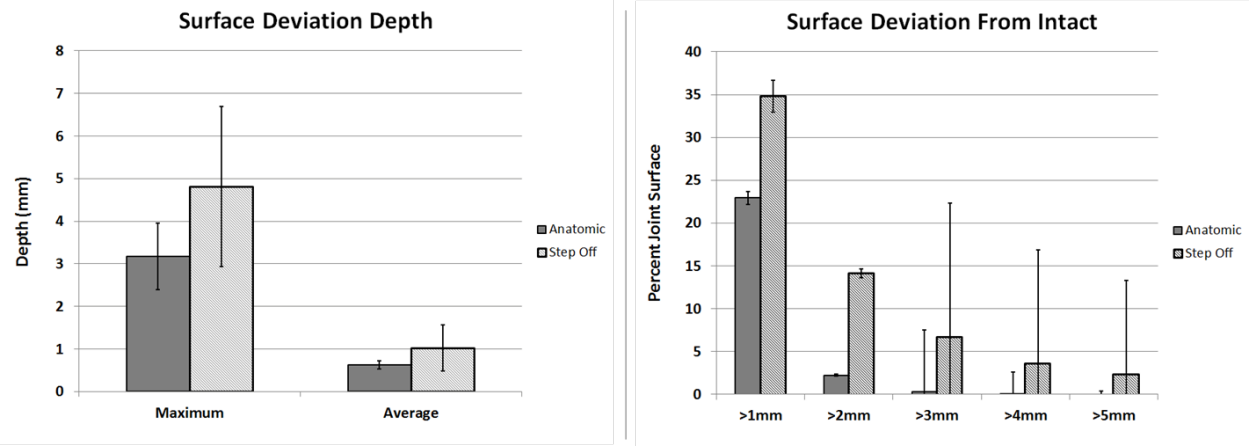

Figure 6. Both the maximum and the average surface depression were higher in animals that were fixed with a 2mm step-off. The step-off animals also demonstrated a much higher amount of total joint surface that was substantially depressed from the intact case, as indicated by the larger bars at the >3mm, >4mm, and >5mm conditions.

2.3.b Experimental Limb Usage

2.3.b.1 Weightbearing Symmetry: A pressure sensing walkway system (Tekscan Inc., North Boston, MA) was utilized for evaluation of the side-to-side asymmetry of hind-leg usage during walking. Each animal was subjected to footprint contact stress measurement prior to the fracture insult (baseline), as well as at 1, 2, 4, 8, and 12 weeks after index surgery. Peak contact stress and vertical impulse was extracted for both the operated left hind-leg and the uninjured right hind-leg. Hind-leg usage asymmetry was then assessed in terms of the contribution of the experimental (left) hind-leg to total (left plus right) hind leg peak force or vertical impulse.

The leg usage status in all 18 of the 12-week survival animals was characterized by significant load protection of the experimental leg at 1 and 2 weeks after surgery which recovered to near pre-operative levels at 4 weeks. The average peak vertical force in the operated limb decreased to 27% of normal (50%) at one week post operatively, and remained decreased to 31% at two weeks post-operatively. By four weeks post-op, and for the duration of the 12-week survival time, peak vertical force returned to 40%-45%. A similar trend was evident in the peak impulse data (Figure 7).

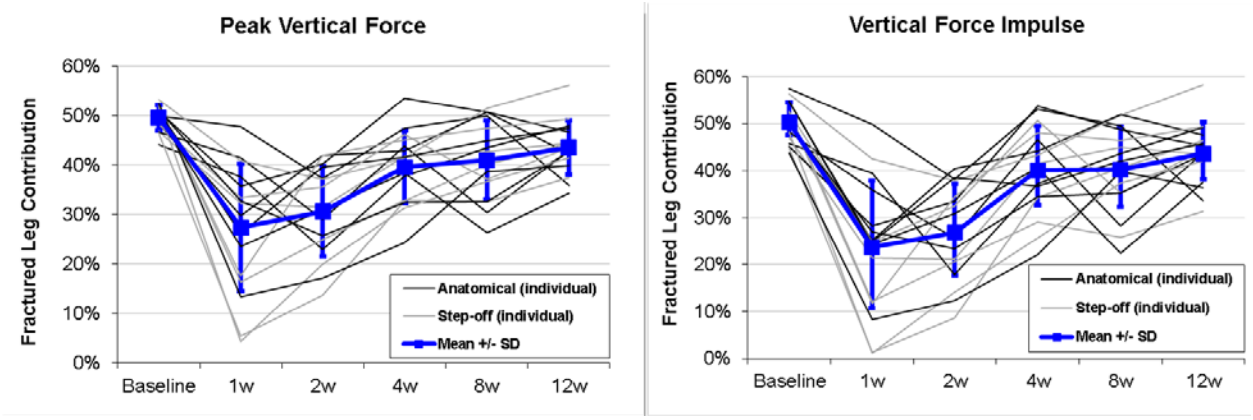

Figure 7. Symmetry of hind-leg loading after experimental intra-articular fracture. The peak vertical force was significantly lower at 1 week ($p<0.001$) and 2 weeks ($p<0.001$), and recovered to similar levels by 4 weeks post-operatively. The vertical force impulse demonstrated a similar trend with a significant decrease at the early post-operative time points which began to recover by 4 weeks postoperatively.

2.3.b.2 Animal Activity Analysis: The overall activity of each animal was measured using a light-weight (48g) wireless accelerometer device developed for monitoring human limb activity (DigiTrac®, IM Systems, Inc. Baltimore, MD). This device reports tri-axial acceleration at the site to which the device is attached. The accelerometer was worn by each of the 12-week survival animals for 6 hours pre-op to establish a baseline activity level, and then again at 1, 2, 4, 8, and 12 weeks to track changes in animal activity. Video recordings were collected at the same time as the accelerometer data. A Matlab routine is being developed to partition the accelerometer data into animal walking (high joint loads), standing (moderate joint loads), and resting/lying down (unloaded) time.

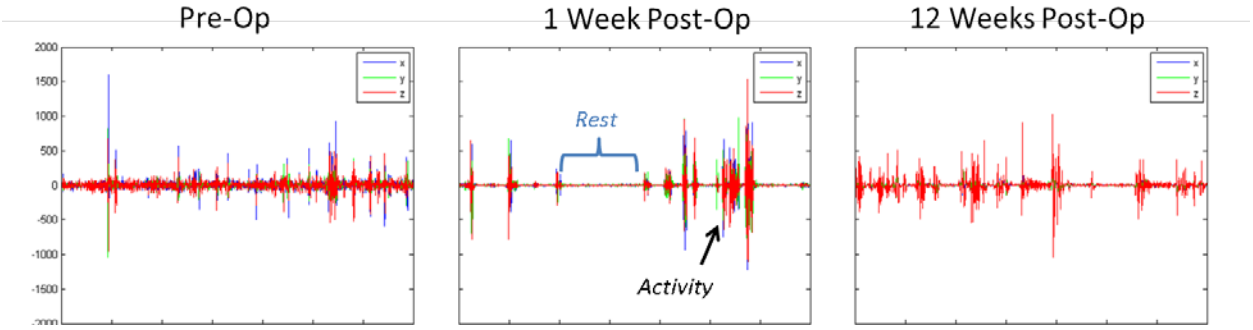

Figure 8. Accelerometer data collected from a single animal at three different time points. There was more activity during the pre-op data collection period than 1 week after intra-articular fracture. 12 weeks post-op, the activity levels were increased, but not yet returned to the pre-op values.

2.3.c Inflammatory Cytokine Response to Intra-articular Fracture

A porcine multiplex cytokine array (Raybiotech, Norcross GA) was used to measure concentrations of ten cytokines (IL1β, IL4, IL6, IL8, IL10, IL12, GMCSF, INFγ, TNF and TGFβ) from the synovial fluid drawn from the fractured and surgically repaired hock and from the non-injured contralateral hock. Interleukin 6 (IL6) and interleukin 8 (IL8) concentrations increased

significantly (Figure 9) in the injured hock at the Day-3 and Week-1 time points ($p<0.001$ for both IL6 and IL8 at both time points). IL6 is an important factor for immune cell signaling during an acute inflammatory response and can function as either a pro- or as an anti-inflammatory factor. IL8 is a pro-inflammatory cytokine that promotes neutrophil chemotaxis and activation, thereby propagating an inflammatory response. Both IL6 and IL8 have been measured at significantly higher levels in synovial fluids of OA patients[3] and in patients with an acute ACL tear.[4] The similar increase in IL6 and IL8 levels in the mini-pig model indicate that there is an equivalent biological response (namely cytokine mediated inflammation) occurring in the acute post-fracture period. Increased levels of IL6 and IL8 have been attributed to an increased concentration of IL1,[3] however the slight increase in IL1β we measured did not reach statistical significance and may not have been related to the measured changes in IL6 and IL8.

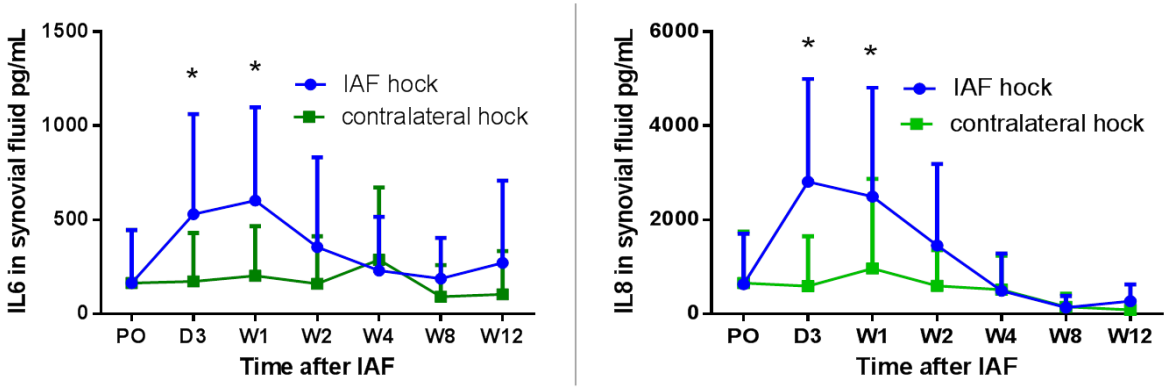

Figure 9. Variation in IL6 and IL8 concentrations with post-operative time. Both IL6 and IL8 concentrations increased significantly from pre-op values (PO) at 3 days (D3) and 1 week (W1) post-operatively. While the IL8 values returned to normal values at the end of the 12-week survival period, IL6 values remained slightly elevated. Asterisks indicate significant differences from baseline values at $p<0.05$.

The concentrations of the other cytokines measured were also not statistically significantly different from pre-operative values at any post-operative time points. However, these non-significant results did show trends toward injury-related increases in TGFβ, IL4, and TNF, and injury-related decreases in IL10. As IL1 and TNF are the primary cytokines that have been associated with cartilage catabolism in the development of OA, the slight increases in mini-pig synovial cytokine concentrations lend further support to a human-like biological response leading to PTOA occurring in the mini-pig hock after joint injury. These inflammatory cytokine data will be correlated with histologically derived information about OA progression in the cartilage and used to generate a full-length manuscript in the coming project year (PY4).

2.3.d Histological Outcomes

At the end of testing period (12 weeks after index surgery), the experimental joints are dissected and prepared for histological evaluation of articular cartilage condition. The specimens are processed following the OARSI guidelines,[5] and sagittal sections from both the medial and lateral tibial and talar surfaces are stained with Safranin-O/Fast Green.

All histological sections from the 12-week survival animals have been generated. The sections are in the process of being digitized for automated Mankin analysis[6] of the extent of

osteoarthritis present 12 weeks after injury. On the fracture-healed tibial surface, distinct proteoglycan (PG) depletion was observed in the vicinity of the fracture line. In the step-off reduced joint, the anterior malleolar step-off surface was covered by fibrous cartilage. Interestingly, the region on the opposing talar cartilage also exhibited PG depletion. The single case of delayed union also exhibited distinctly greater PG depletion than any of the well-healed joints (anatomic or step-off).

The normal appearance of Yucatan mini-pig cartilage is in the process of being catalogued from normal, non-injured animals to provide mini-pig-specific Mankin scoring parameters and establish a normal baseline appearance for healthy cartilage. Specifically, the thickness of each cartilage zone (superficial, transitional, radial, and deep), and the cell density and PG staining intensity in each zone are being measured from normal, non-injured animals. The automated Mankin scoring program will then be run on the histological sections from each experimental animal, yielding continuous quantitative measures of cell density and PG distribution. These continuous measures will be interpreted against the normal mini-pig values to obtain a species-specific Mankin score of OA severity.

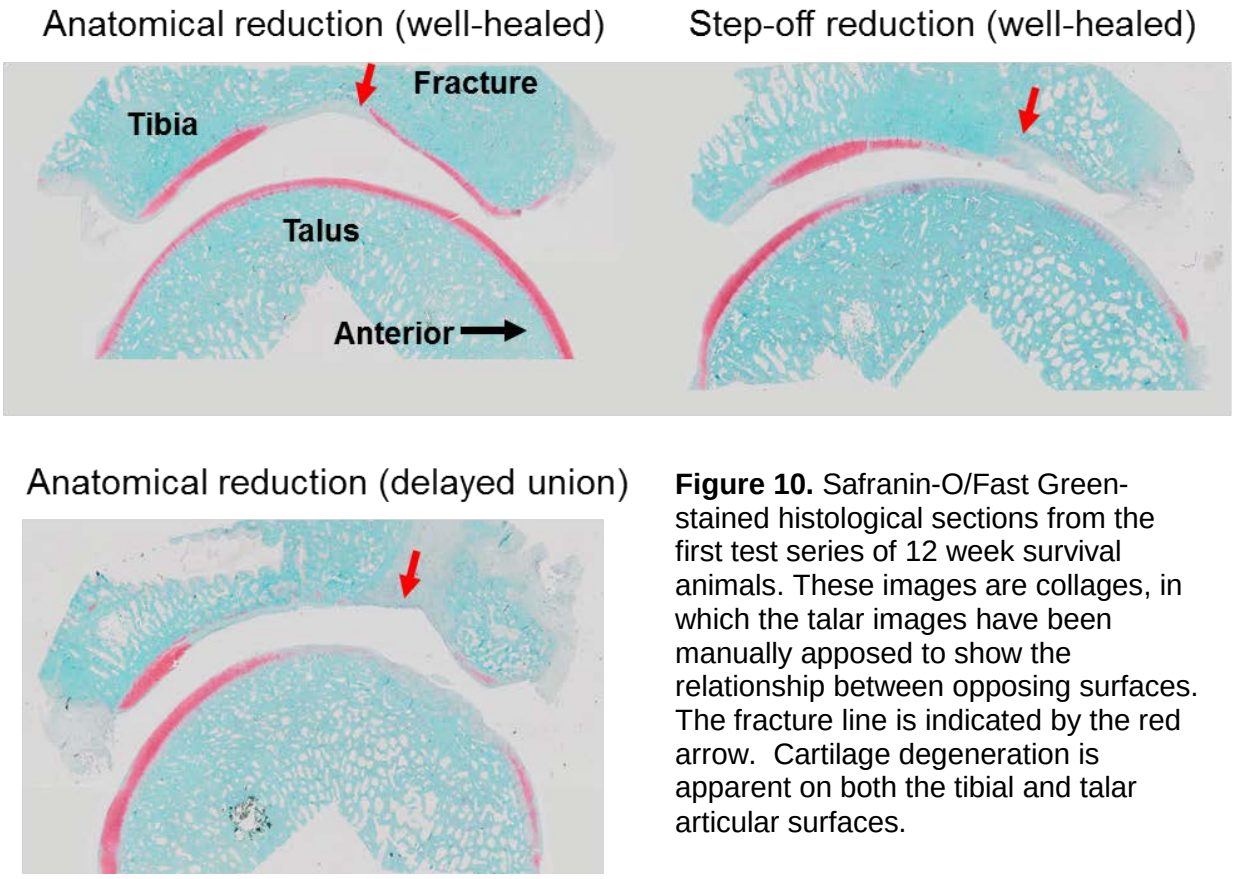

Figure 10. Safranin-O/Fast Green-stained histological sections from the first test series of 12 week survival animals. These images are collages, in which the talar images have been manually apposed to show the relationship between opposing surfaces. The fracture line is indicated by the red arrow. Cartilage degeneration is apparent on both the tibial and talar articular surfaces.

2.3.e Tasks 2 & 3 Progress Summary

During PY3, the 12-week survival experimental surgeries using the definitive fracture and subsequent fixation protocols were completed. The mechanical data analysis is completed (limb-loading and joint congruity) or nearly completed (animal activity). The biological analysis is complete (inflammatory cytokines), and the final step remaining for PY4 is the analysis of the

newly available histological slides. These data will be compiled into full-length manuscripts in PY4.

2.4 Task 4 – Demonstration of Model Utility

Aim 3 of this project is to demonstrate the utility of the mini-pig model as a pre-clinical tool in which to evaluate promising treatments to prevent PTOA following intra-articular fracture. In the original statement of work, OP-1/BMP-7 was proposed as the treatment that would be used to reduce inflammation in the acute period following intra-articular fracture. In the revised statement of work associated with the change in PI, OP-1/BMP-7 was replaced with a cocktail of glycyrrihizin (GZ) and n-acetyl cystine (NAC). Glycyrrihizin is an anti-inflammatory, and NAC is an antioxidant. The cocktail has shown great promise for reducing inflammation in smaller animal models, and like OP-1/BMP-7, both NAC and GZ are approved for use in humans. This cocktail serves the same purpose in the mini-pig model of reducing inflammation, and presents a more interesting research target as this pairing is a novel combination of therapeutics. The NAC/GZ compound is administered as intra-articular injection with the treatments suspended in a hyaluronic acid hydrogel which becomes more viscous at body temperature and prevents the therapeutics from leaking out of the injured joint.

Due to Dr. Tochigi's departure, there was a delay in completing the 30 animal surgeries associated with this Aim. Dr. Tochigi had been the surgeon performing the steps to apply the hardware devices required to create the intra-articular fracture. Dr. Bergh, previously the veterinary consultant on the project, became the primary surgeon upon Dr. Tochigi's departure. However Dr. Bergh lives in Ames, Iowa, and had to commute to Iowa City to perform surgeries, which greatly slowed the progress completing the experiments to address this final Aim. Of the 30 total animals proposed to address this Aim, in PY3, 3 animals with IAF and no treatment (hydrogel injection only), 3 animals with IAF and the NAC/GZ treatment, and 3 sham animals (with all surgical steps and no IAF) have been completed. The remaining 21 animals will be completed early in PY4 to ensure adequate time to evaluate the results before the end of the project extension.

2.4.a Histological Analysis of Inflammation

In the short 1-week survival time of the animals associated with this Aim, there is not enough time for dramatic changes to occur in the cartilage. Inflammation typically appears in the soft tissues surrounding the joints earlier than in the cartilage matrix. Therefore, in addition to cartilage histology and the other outcomes developed for the investigation of Aims 1 and 2, we collected synovial tissue from the posterior medial and lateral sides of the hock. Because the goal of this aim is to demonstrate a reduction of inflammation with treatment following intra-articular fracture, the synovium was processed into histological sections and evaluated for signs of inflammation.

The digitized histological sections are evaluated automatically using a custom routine developed in Visiomorph software (Visiopharm Inc., Hoersholm, Denmark). Based on staining color, cell nuclei, fibrous tissue, and fat cell areas are automatically identified. After a series of morphological evaluations to differentiate between tissue and cell types, the density of monocytes in the fatty tissue and the ratio of fibrous tissue to the total tissue area are calculated. Increased monocyte density and increased fibrous tissue area are hallmarks of inflammation. This routine will be used to directly assess the effects of the anti-inflammatory treatment administered during Aim 3 experiments.

Due to the limited number of Aim 3 surgeries that could be completed in PY3, and the normal period of time associated with histological processing, only one synovial specimen has been available for analysis. However, this routine has proven effective for discerning differences between inflamed synovial tissues harvested from smaller animal models. As the histological samples from the 9 completed and the 21 remaining Aim 3 experiments become available, this method will be used to directly quantify the anti-inflammatory effects of the therapeutics being investigated in this mini-pig model.

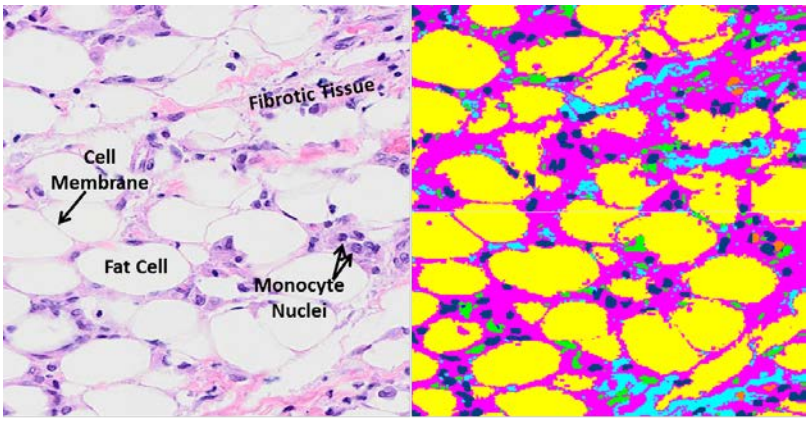

Figure 11. Hematoxylin and eosin-stained synovial tissue from a rabbit (left) and the corresponding analysis performed in Visiomorph (right). Cell nuclei (blue), fat cell area (yellow), fibrous tissue (cyan) and membranous tissue (magenta) are automatically identified and used to quantify extent of inflammation.

2.4.b Oxidative Stress Measurement

Glutathione (GSH) is a tripeptide thiol, which acts as the primary redox buffer of the cell. The ratio of GSH to its oxidized counterpart, glutathione disulfide (GSSG), is an indication of the oxidative stress of cell. Specifically, the ratio of GSSG/total GSH will increase in cells that are oxidatively stressed. Since intra-articular fracture introduces a large amount of excess oxygen into the joint (primarily via blood entering the joint), which could contribute to oxidative stress in the cartilage after IAF, and because one of the functions of NAC is to act as an anti-oxidant and decrease oxidative stress that may damage the cartilage, measurement of this ratio is of interest in the Aim 3 experimental animals. Immediately after sacrifice and prior to fixation for histological analysis, a small cartilage sample is excised from the joint surface for analysis of the GSSG/GSH content via the method of Griffith.[7] In the nine completed animal experiments, it was found that intra-articular fracture without any treatment (hydrogel vehicle injection only) resulted in an increase in oxidative stress in the cartilage. Administration of NAC/GZ treatment immediately following intra-articular fracture was able to return the increased GSSG/GSH ratio to baseline levels. While these results are a promising indication of the ability of the NAC/GZ treatment to help treat cartilage following an intra-articular fracture, these results are only from a small number of animals. These early results will be explored further during PY4 with the addition of samples from the remaining animal experiments in Aim 3.

3. KEY RESEARCH ACCOMPLISHMENTS DURING PY3

- Completion of 12-week survival experimental series
- Confirmation of radiographic fracture healing in a time course very consistent with the post-injury time course of human clinical IAFs
- Confirmation of gradual recovery of experimental joint loading

- Confirmation of an inflammatory cytokine response following joint injury similar to that seen in human joint injury
- Confirmation of cartilage histological findings consistent with human post-traumatic OA
- Application of a CT-based image analysis technique enabling quantitative evaluation of joint incongruity in the fractured experimental joints
- Early indications of the utility for this porcine model of intra-articular fracture to demonstrate therapeutic effects of anti-inflammatory treatment in the acute post-injury period

4. REPORTABLE OUTCOMES

4.1 Peer-reviewed Papers

- Tochigi Y, Buckwalter JA, Martin JA, Hillis SL, Zhang P, Vaseenon T, Lehman AD, Brown TD. *Distribution and progression of chondrocyte damage in a whole-organ model of human intra-articular fracture.* J Bone Joint Surg Am. 2011 Mar;93(6):533-9.
- Tochigi, Y; Zhang, P; Rudert, MJ; Baer, TE; Martin, JA; Hillis, SL; Brown, TD. *A novel impaction technique for modeling intra-articular fracture in large animal joints.* Osteoarthritis Cartilage 2013; 21(1): 200-8.
- Diestelmeier BW, Rudert MJ, Tochigi Y, Baer TE, Fredericks DC, Brown TD. *An instrumented pendulum system for measuring energy absorption during fracture insult to large animal joints in vivo.* J Biomech Eng. (In Press).

4.2 Meeting Abstracts/Presentations

- Diestelmeier, BW; Rudert, MJ; Tochigi, Y; Baer, TE; Fredericks, DC; Brown, TD. *Quantification impaction system for a large animal survival model of intraarticular fracture.* 36th Annual Meeting of the American Society of Biomechanics, August 15–18, 2012, Gainesville, Florida.
- Tochigi, Y; Diestelmeier, BW; Rudert, MJ; Baer, TE.; Fredericks, DC.; Arunakul, M; Brown, TD. *A clinically-realistic large animal survival model of human intra-articular fracture.* 2013 Annual Meeting of the Orthopaedic Research Society, January 26–29, 2013, San Antonio, Texas. Paper #0138, Session 023:
- Swanson, E; Goetz, JE; Tochigi Y. *Evaluation of articular surface geometry deviation and cartilage damage in a porcine model of intra-articular fracture.* 2013 Annual Meeting of the Orthopaedic Research Society, January 26–29, 2013, San Antonio, Texas. Poster #PS1-056.
- Roberts N, Martin JA, Fredericks DC, Tochigi Y, Goetz JE. Fluctuation of synovial fluid inflammatory cytokine concentrations in an animal model of intra-articular fracture. 2014 Annual Meeting of the Orthopaedic Research Society, March 15-18, 2014, New Orleans, LA. (submitted)
- Coleman MC, Fredericks DC, Martin JA, Goetz JE. *Intraarticular administration of n-acetyl cysteine and glycyrrhizin alleviates acute oxidative stress following intraarticular fracture.* 2014 Annual Meeting of the Orthopaedic Research Society, March 15-18, 2014, New Orleans, LA. (submitted)

4.3 Degrees Obtained

- *Design and application of an instrumented pendulum device for measuring energy absorption during fracture insult in large animal joints in vivo.* M.S. thesis, Bryce W. Diestelmeier, Department of Biomedical Engineering, The University of Iowa, 2012.

4.4 Research Grants (funded)

- US Department of Defense (Department of Army) CDMRP-PRMRP
  Technology/Therapeutic Development Award W81XWH-11-1-0583
  Mitochondrial Based Treatments that Prevent Posttraumatic Osteoarthritis in a Translational Large Animal Intraarticular Fracture Survival Model
  (PI: Todd O. McKinley, MD)
- NIH/NIAM CORT Grant 5 P50 AR055533
  Innovations to Assess and Forestall Post-Traumatic Osteoarthritis
  (Program Director: Joseph A. Buckwalter, MD)
  Project-2: Establishing Treatments and Diagnostic Tools for Post-Traumatic OA In Vivo.
  (Project PI: Yuki Tochigi, MD, PhD)

5. CONCLUSION

As reported above, our PY3 work used the definitive modeling protocol finalized in PY2 to complete 12-week survival animal surgeries required to address Specific Aims 1 & 2. Analysis of the resulting data is nearly complete, with only the histological analysis remaining. Accordingly, Milestone #4 is nearly achieved, with abstracts submitted to the Orthopaedic Research Society documenting the natural course of the fractured and repaired mini-pig hock joint. That milestone will be fully achieved once the histological data are fully analyzed and the entire body of data is compiled into a full-length manuscript.

Despite delays associated with the departure of Dr. Tochigi, we have begun the experimental surgeries to address Aim 3 and Task #4 in the SOW. Early indications are that the new combination of NAC/GZ (anti-oxidant/anti-inflammatory) treatment is capable of providing some level of protection to the insulted joint in terms of inflammation reduction in the synovium and oxidative stress reduction in the cartilage.

During PY4, the natural course of intra-articular fracture in the porcine model will be published. Simultaneously, the experimental surgeries to finish Aim 3 will be completed and the data will be analyzed to demonstrate the ability of the porcine model to serve as a pre-clinical model for human-relevant pharmacological interventions (Task 4).

6. REFERENCES

1. Diestelmeier, BW. 2012. Design and application of an instrumented pendulum device for measuring energy absorption during fracture insult in large animal joints in vivo. M.S. thesis, Department of Biomedical Engineering, The University of Iowa, 2012.
2. Tochigi, Y; Zhang, P; Rudert, MJ; Baer, TE; Martin, JA; Hillis, SL; Brown, TD. A novel impaction technique for modeling intra-articular fracture in large animal joints. Osteoarthritis and Cartilage 2013; 21(1): 200-8.
3. Cameron ML, Fu FH, Paessler HH, Schneider M, Evans CH. Synovial fluid cytokine concentrations as possible prognostic indicators in the ACL-deficient knee. Knee Surg, Sports Traumatol, Arthroscopy. 1994; 2: 38-44.

4. Swärd P, Frobell R, Englund M, Roos H, Struglics A. Cartilage and bone markers and inflammatory cytokines are increased in synovial fluid in the acute phase of knee injury (hemarthrosis) - a cross-sectional analysis". Osteoarthritis and Cartilage, 2012; 20(11): 1302-8.
5. Pritzker KP, Gay S, Jimenez SA, Ostergaard K, Pelletier JP, Revell PA, Salter D, van den Berg WB. Osteoarthritis cartilage histopathology: grading and staging. Osteoarthritis and Cartilage. 2006; 14(1): 13-29.
6. Moussavi-Harami SF, Pedersen DR, Martin JA, Hillis SL, Brown TD. Automated objective scoring of histologically apparent cartilage degeration using a custom image analysis program. J Orthop Res. 2009; 27(4): 522-8.
7. Griffith OW. Determination of glutathione and glutathione disulfide using glutathione reductase and 2-vinylpyridine. Anal Biochem 1980; 106(1): 207-12.

An Instrumented Pendulum System for Measuring Energy Absorption During Fracture Insult to Large Animal Joints *In Vivo*

Diestelmeier B W[3], Rudert M J[1], Tochigi Y[4], Baer T E[1], Fredericks D C[1], Brown T D[1,2]
Departments of [1]Orthopaedics and Rehabilitation and [2]Biomedical Engineering, University of Iowa, Iowa City, IA, [3]current address Boston Scientific, Minneapolis, MN, [4]current address Department of Orthopaedics, Dokkyo Medical University Koshigaya Hospital, 2-1-50 Minamikoshigaya, Koshigaya, Saitama, 343-8555, Japan

Abstract

Background: For systematic laboratory studies of bone fractures in general, and intra-articular fractures in particular, it is often necessary to control for injury severity. Quantitatively, a parameter of primary interest in that regard is the energy absorbed during the injury event. For this purpose, a novel technique has been developed to measure energy absorption in experimental impaction. The specific application is for fracture insult to porcine hock (tibio-talar) joints *in vivo*, for which illustrative intra-operative data are reported.

Method of Approach: The instrumentation allowed for the measurement of the delivered kinetic energy and of the energy passed through the specimen during impaction. The energy absorbed by the specimen was calculated as the difference between those two values. A foam specimen validation study was first performed to compare the energy absorption measurements from the pendulum instrumentation versus the work of indentation performed by an MTS machine. Following validation, the pendulum apparatus was used to measure the energy absorbed during intra-articular fractures created in fourteen minipig hock joints *in vivo*.

Results: The foam validation study showed close correspondence between the pendulum-measured energy absorption and MTS-performed work of indentation. In the survival animal series, the energy delivered ranged from 31.5 to 48.3 joules (41.3 ± 4.0, mean ± sd), and the proportion of energy absorbed to energy delivered ranged from 44.2% to 64.7% (53.6% ± 4.5%).

Conclusions: The foam validation results support the reliability of the energy absorption measure provided by the instrumented pendulum system. Given that a very substantial proportion of delivered energy passed - unabsorbed - through the specimens, the energy absorption measure provided by this novel technique arguably provides better characterization of injury severity than is provided simply by energy delivery.

Introduction

Biomechanical impaction experiments have often been performed to study tissue and organ responses to injury (e.g., [1-5]). In the field of orthopaedic biomechanics, fractures of bone are of particular interest. Clinically, the severity of fractures is often (subjectively) described in terms of the energy of the precipitating injury event [6]. Among fractures of bone, those involving the joint surface (intra-articular fractures, IAFs) are especially challenging from an orthopaedic management standpoint [7]. Besides fostering bony healing, treatment also aims to forestall post-traumatic osteoarthritis (PTOA), joint deterioration which arises from chronic loading abnormality of imprecisely reduced fractures, and/or from acute insult of cartilage. To date, IAFs have received relatively little attention in controlled laboratory settings. Rather, most research on IAFs has involved either registry-based clinical studies [8-11], or laboratory animal or cadaveric models where the insult of interest (e.g., osteotomy [12-15]) bears only limited similarity to an actual physiologic IAF event.

For systematic laboratory studies of bone fractures in general, and IAFs in particular, it is necessary to control for injury severity. Quantitatively, a parameter of primary interest in that regard is the energy absorbed during the fracture event [16]. Normally, however, energy assessments in laboratory injury models have involved only the energy delivered to the specimen [1, 2], rather than the energy actually absorbed in the injury.

This paper reports novel methodology for measuring the fracture energy absorbed in laboratory biomechanical impaction experiments. The specific implementation is in a testing system used to create IAFs in a large-animal survival model, the porcine hock joint [17]. The underlying concept, however, is generalizable to a wide variety of laboratory impaction experiments.

Methods

Impacts were delivered by a novel instrumented pendulum system (Figure 1A) designed for survival animal studies, and capable of delivering energy levels sufficient to fracture major weight-

bearing joints in large species. The system, shown diagrammatically in Figure 1B, is compatible with operating room sterile field conditions required for survival studies. Employing the principle of the standard Charpy and Izod impact energy tests [18], energy delivery to the joint is modulated by controlling the release height of a pendulum. When using porcine (minipig) hock joints to model human tibial pilon fractures, the study animal's talus and tibia are suspended in appropriate apposition for creating fractures of the distal tibial articular surface, using a previously described purpose-designed bone anchoring apparatus (Figure 1C). To increase experimental reproducibility of fracture morphology, a sub-articular surface stress-rising crack (saw cut) is employed [17]. The apparatus is mounted in series with a sled that can translate horizontally along low-friction linear bearings. Translation of the sled from the impact position is resisted by a linear compression spring, placed between the sled and a fixed stop.

The instrumentation for energy absorption measurement is based on the concept that not all of the energy delivered by the pendulum mass will be absorbed by the joint during the fracture event [19]. While the pendulum itself would not "swing through" the specimen as happens in an Izod or Charpy test, nevertheless, a substantial portion of the delivered energy will pass through the specimen, and will be absorbed elsewhere, in series, by the overall testing set-up. If this through-passed energy could be measured, the difference between the delivered energy and the through-passed energy would correspond to the energy absorbed in the specimen. In the pendulum system, the magnitude of energy delivery ($KE = \frac{1}{2}mv^2$) is calculated from the pendulum mass (6.1 kg) and its linear velocity, v, at impact, where linear velocity is derived from the product of angular velocity (measured by a potentiometer at the pendulum pivot) times the length of the pendulum arm. Use of the kinetic energy as the delivered energy, rather than its nominally equivalent potential energy ($PE = mgh$), corrects for friction losses at the pendulum arm pivot bearing. The mass of the pendulum arm (0.80 kg), distributed uniformly along its 1.0-m length, is neglected; thus, the actual delivered kinetic energy may be slightly greater than the value calculated using the pendulum mass only.

For setup of the system prior to a test, the specimen tripod support is positioned on the sled such that, at impact, the pendulum will be exactly vertical (i.e., KE is maximum), the sled stationary, and the spring uncompressed. The pendulum mass is then raised to a predetermined height and released. The mass impacts the tripod anchor, driving the talus into and fracturing the tibia [17]. During the fracture event, the spring acts to decelerate the sled from its immediately-post-impact velocity, until bringing it to a stop. A linear potentiometer mounted in parallel with the sled measures the sled's maximum displacement, x, at the instant of stopping. The through-passed energy (i.e., the energy transferred from the specimen to the sled) is calculated by $TE = \frac{1}{2}kx^2$, where k is the spring constant. Raw analog voltage signals from the angular (pendulum) and linear (sled) potentiometers are digitized at 15 kHz using LabVIEW, and converted into energy data using a custom MATLAB script. The difference between (pre-impact) kinetic energy of the pendulum mass and the through-passed energy transferred to the sled is thus the specimen's absorbed energy AE: AE = KE – TE.

To validate the energy absorption measurements, a polymer foam surrogate for what would otherwise be a minipig hock joint was utilized. A necessary characteristic of this surrogate material was that its energy absorption properties be uniform and measurable. Based on previous empirical experience [16], rigid polyurethane foam (25 lb/ft^3 density, Last-a-Foam, General Plastics Mfg. Co., Tacoma, WA) was chosen. Eighteen identically sized blocks (5.5 x 5.5 x 4.0 cm) of the foam were cut and impact-tested with the pendulum system. Rather than employ the tripod mounting fixture used to test animal joints, each foam block rested on the smooth surface of the sled, in contact with a rigid, flat-ended cylindrical indenter (11.7 mm diameter) which was in turn rigidly affixed to the sled (Figure 2). Trial-and-error with different-sized indenters was used to find the largest diameter that would create an easily detected and measured indentation (depth > 0.50 mm) at the lowest impact energy. As with the hock joint fracture tests, the pendulum mass was raised and released, for this test configuration driving the block into the indenter. The digitized linear and rotary potentiometer signals were used to determine the impact duration, which was measured from the initial contact (pendulum

vertical) until the time when the pendulum and sled-mounted indenter moved in unison, i.e., when no further penetration of the indenter occurred. For the impacts, durations ranged from approximately 20 msec to 40 msec. Six blocks were tested at each of three different pendulum drop heights (input KE), corresponding to 20^{o}, 40^{o}, and 60^{o} pendulum release angles, and the absorbed energy (AE) was calculated for each test. The depth of indenter penetration for each impact was subsequently measured using a digital caliper (± 0.01 mm).

To provide a "gold standard" independent measurement of energy absorption of the foam, the same indenter (removed from the pendulum system sled) was mounted to an MTS servohydraulic test machine's actuator. Each of the eighteen previously pendulum-impacted blocks was supported on the MTS load cell, and the indenter was driven into the block at a site adjacent to that of the pendulum impact. The actuator was displacement-control programmed to nominally apply similar penetration depths as those obtained with the pendulum. The full penetration depth was reached via a 50-msec linear ramp in all tests, the maximum rate obtainable while maintaining closed-loop stability. Although this was slightly longer than the pendulum impact durations, experimentation at other rates showed no evidence of significant rate-dependency. All indentation depths were directly caliper-measured and absorbed energies were determined via integration of the MTS load-displacement curves.

Following the system validation tests, a preliminary series of cadaveric hock specimen experiments was conducted to determine appropriate parameters (e.g., pendulum mass, drop height, length and stiffness of the compression spring) required to achieve bone fracture. Four representative tibial plateau fractures from the cadaver series are shown in Figure 3. They exhibit the general clinical appearance of human fractures - the primary fracture lines are medial-lateral and an intact anterior fragment of less than one-half of the total articular surface area is minimally displaced. After the parameters were established, the pendulum impaction system was used in an institutionally

approved (IACCUC #1007141) survival animal study, in which experimental IAFs were created in fourteen minipig hocks *in vivo* (approximate age two years, weight 90 kg).

Results

Results of the foam surrogate tests for eighteen blocks are summarized in Table 1. They were pendulum-impacted, six blocks at each of three release heights, absorbed energies were calculated, and the penetration depths were caliper-measured after each test. The blocks were then MTS-impacted under displacement control, with the target penetration depth for each group set to the average depth obtained in the pendulum impacts - the actual penetration depths reached were directly caliper-measured. Absorbed impact energies for both impact types were plotted vs. penetration depths and linear regressions showed strong correlations (Figure 4). Pendulum-impact absorbed energy vs. MTS-impact absorbed energy is plotted in Figure 5.

Pendulum system energy results for the fourteen individual live-animal hock joint fractures are reported in Table 2. Energy delivered (KE) ranged from 31.5 to 48.3 joules (41.3 ± 4.0, mean ± sd). The low delivered energy for animal number one (31.5 J) was due to a lower pendulum drop height used for that specimen only. Through-passed energy (TE) ranged from 14.7 to 21.8 joules (19.0 ± 1.9), and absorbed energy (AE) ranged from 16.9 to 28.3 joules (22.2 ± 3.5). The proportion of absorbed energy to energy delivered ranged from 44.2% to 64.7% (53.6% ± 4.5%). Absorbed energy vs. delivered energy is plotted in Figure 6.

Discussion

The instrumented pendulum impaction system documented in the present study measures the magnitude of energy absorption during experimental impaction, in terms of the difference between

the delivered and through-passed energy magnitudes. To our best knowledge, this system is the first to enable energy absorption measurement in biomechanical impaction settings.

For the foam surrogate validation study, pendulum-absorbed energies were slightly greater than MTS-absorbed energies, for similar penetration depths, particularly at the highest delivered energy (Table 1 and Figure 5). This was not unexpected, as the pendulum device accounts for energy absorbed by the entire system, including penetration, friction, and deflection or vibration of the (non-spring) components of the pendulum device itself, whereas the MTS test isolates the energy expended only in penetration. The non-penetration absorbed energy effects in the pendulum device may become larger with higher delivered energies. However, the generally good agreement between the pendulum-determined absorption energy and the MTS-determined absorption energy suggests that such energy losses are minor.

As is apparent from the results of the survival-animal pendulum-induced fractures (Table 2), only a portion (53.6%) of the delivered energy was absorbed in creating the experimental injury, while a significant amount (46.4%) passed through the hock specimen, subsequently being absorbed in spring compression. The relationship between absorbed and applied energy is linear (Figure 6). However, caution is urged in applying this relationship to other fracture studies. In the present fracture impaction setting, there can be a variety of factors that contribute to energy absorption during an impaction event, including non-bone-fracture factors such as soft tissue damage/deformation. The current technique does not permit discriminating the energy absorption directly associated with bony fracture versus these non-fracture factors. (Imaging techniques for estimating bone fracture energy from CT-based assessment of *de novo* inter-fragmentary free surface area have recently been developed [20], but are outside the scope of the present study.) However, the present survival experiment results indicate that, at least in this range of impaction parameters for this particular surgical preparation, delivered energy is clearly not a sufficient measure of the energy actually absorbed in creating tissue injury.

Presumably, the degree of discrepancy between delivered versus absorbed energy in any given impaction experiment would be specific to considerations such as specimen type, support fixation arrangement, impaction parameters, etc. Nevertheless, the substantial disparity (46.4%) apparent in this particular experimental setting, seemingly at least generally representative of many laboratory biomechanical impaction experiments, serves to vividly illustrate the fallacy of presuming that delivered energy is necessarily representative of the energy actually involved in causing specimen tissue damage. The sled-spring arrangement used in this particular experimental setting arose as an outgrowth of an already-in-use impaction system. Obviously, however, a wide variety of similarly conceived instrumentation designs might well be used to implement the same underlying concept, in other specific study designs.

While it might be possible to design/perform experiments where absorbed energy much more closely approximates delivered energy (based on empirical trials), biologic variability is such that many such trials might fail to produce bony fracture, thus requiring (biologically-confounding) repeat impactions. So, for practical purposes, it is desirable to deliver kinetic energy levels that are amply large to reliably achieve fracture, which in turn presumes that through-passed energy levels will in general be non-negligible.

Acknowledgements

This research was supported by NIH CORT grant P50 AR055533 and DOD grants W81XWH-10-1-0864 and W81XWH-11-1-0583.

References

[1] Backus JD, Furman BD, Swimmer T, Kent CL, McNulty AL, Defrate LE, Guilak F, Olson SA. Cartilage viability and catabolism in the intact porcine knee following transarticular impact loading with and without articular fracture. Orthop Res. 2011 Apr;29(4):501-510.

[2] Tochigi Y, Buckwalter JA, Martin JA, Hillis SL, Zhang P, Vaseenon T, Lehman AD, Brown TD. Distribution and progression of chondrocyte damage in a whole-organ model of human ankle intra-articular fracture. J Bone Joint Surg Am. 2011 Mar 16; 93(6):533-539.

[3] Borrelli J Jr, Burns ME, Ricci WM, Silva MJ. A method for delivering variable impact stresses to the articular cartilage of rabbit knees. J Orthop Trauma. 2002 Mar;16(3):182-188.

[4] Isaac DI, Meyer EG, Haut RC. Chondrocyte damage and contact pressures following impact on the rabbit tibiofemoral joint. J Biomech Eng. 2008 Aug;130(4):041018.

[5] Rundell SA, Baars DC, Phillips DM, Haut RC. The limitation of acute necrosis in retro-patellar cartilage after a severe blunt impact to the in vivo rabbit patello-femoral joint. J Orthop Res. 2005 Nov;23(6):1363-1369.

[6] Marsh JL, Slongo TF, Agel J, Broderick JS, Creevey W, DeCoster TA, Prokuski L, Sirkin MS, Ziran B, Henley B, Audigé L. Fracture and dislocation classification compendium - 2007: Orthopaedic Trauma Association classification, database and outcomes committee. J Orthop Trauma. 2007 Nov-Dec;21(10 Suppl):S1-133.

[7] McKinley TO, Borrelli J Jr, D'Lima DD, Furman BD, Giannoudis PV. Basic science of intra-articular fractures and posttraumatic osteoarthritis. J Orthop Trauma. 2010 Sep;24(9):567-570.

[8] Saterbak AM, Marsh JL, Nepola JV, Brandser EA, Turbett T. Clinical failure after posterior wall acetabular fractures: the influence of initial fracture patterns. J Orthop Trauma. 2000 May;14(4):230-237.

[9] Lansinger O, Bergman B, Körner L, Andersson GB. Tibial condylar fractures. A twenty-year follow-up. J Bone Joint Surg Am. 1986 Jan;68(1):13-19.

[10] Stevens DG, Beharry R, McKee MD, Waddell JP, Schemitsch EH. The long-term functional outcome of operatively treated tibial plateau fractures. J Orthop Trauma. 2001 Jun-Jul;15(5):312-320.

[11] Marsh JL, Weigel DP, Dirschl DR. Tibial plafond fractures. How do these ankles function over time? J Bone Joint Surg Am. 2003 Feb;85-A(2):287-295.

[12] Trumble T, Verheyden J. Remodeling of articular defects in an animal model. Clin Orthop Relat Res. 2004 Jun;(423):59-63.

[13] McKinley TO, Tochigi Y, Rudert MJ, Brown TD. Instability-associated changes in contact stress and contact stress rates near a step-off incongruity. J Bone Joint Surg Am. 2008 Feb;90(2):375-383.

[14] Lefkoe TP, Trafton PG, Ehrlich MG, Walsh WR, Dennehy DT, Barrach HJ, Akelman E. An experimental model of femoral condylar defect leading to osteoarthrosis. J Orthop Trauma. 1993;7(5):458-467.

[15] Vaseenon T, Tochigi Y, Heiner AD, Goetz JE, Baer TE, Fredericks DC, Martin JA, Rudert MJ, Hillis SL, Brown TD, McKinley TO. Organ-level histological and biomechanical responses from localized osteoarticular injury in the rabbit knee. J Orthop Res. 2011 Mar;29(3):340-346.

[16] Beardsley CL, Anderson DD, Marsh JL, Brown TD. Interfragmentary surface area as an index of comminution severity in cortical bone impact. J Orthop Res. 2005 May;23(3):686-690.

[17] Tochigi Y, Zhang P, Rudert MJ, Baer TE, Martin JA, Hillis SL, Brown TD. A novel impaction technique to create experimental articular fractures in large animal joints. Osteoarthritis Cartilage. 2013 Jan;21(1):200-208.

[18] Callister WDJ. *Materials Science and Engineering: An Introduction*, John Wiley and Sons, New York, New York, 1994.

[19] Abdel-Wahab AA, Silberschmidt VV. Experimental and numerical analysis of Izod impact test of cortical bone tissue. European Physical Journal Special Topics. 2012;206-210.

[20] Thomas TP, Anderson DD, Mosqueda TV, Van Hofwegen CJ, Hillis SL, Marsh JL, Brown TD. Objective CT-based metrics of articular fracture severity to assess risk for post-traumatic osteoarthritis. J Orthop Trauma. 2010; 24(12):764–769.

List of Figures

List of Tables

Figure 1

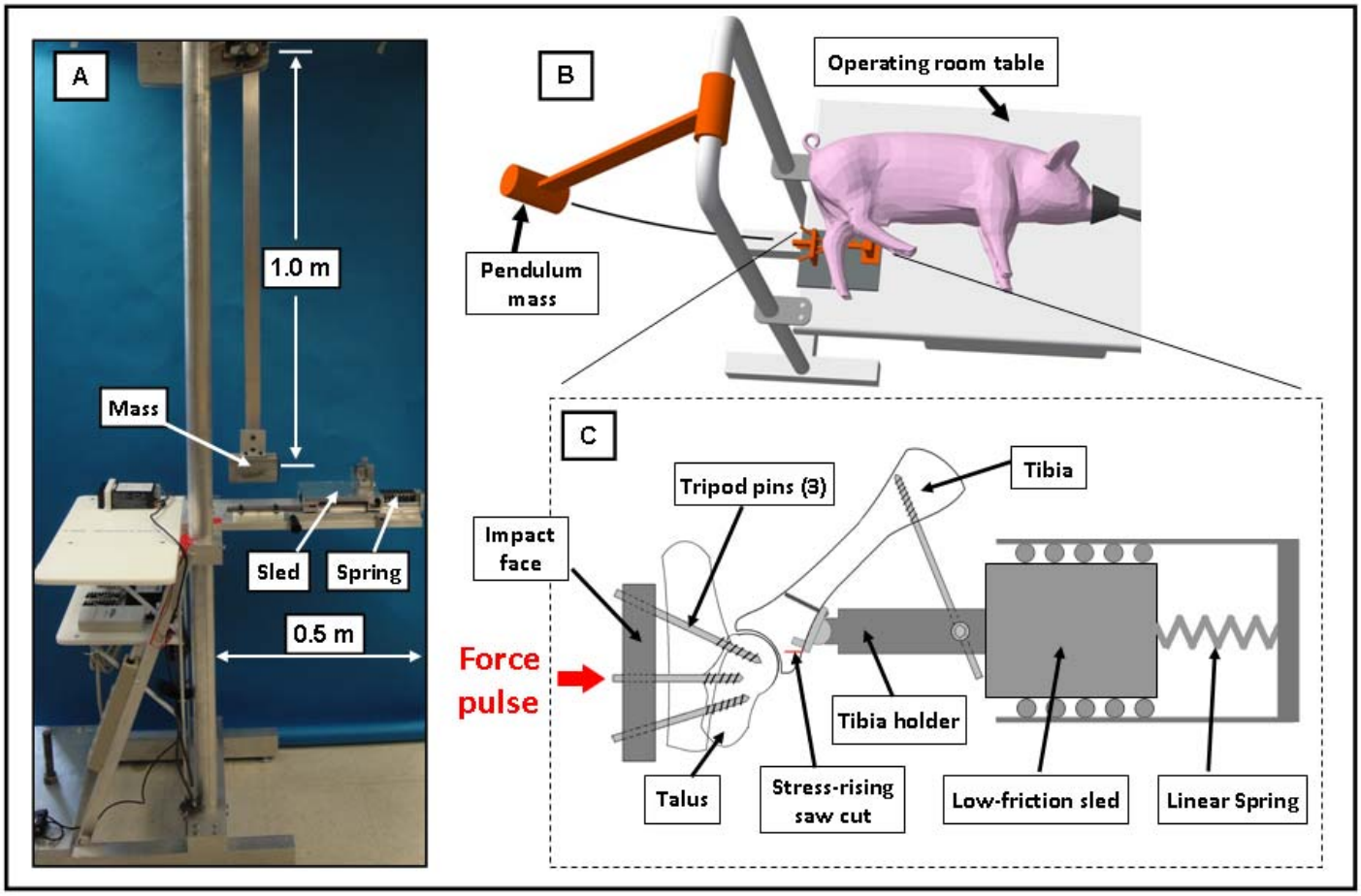
A
1.0 m
Mass
Sled
Spring
0.5 m
B
Operating room table
Pendulum mass
C
Tripod pins (3)
Tibia
Impact face
Force pulse
Tibia holder
Talus
Stress-rising saw cut
Low-friction sled
Linear Spring

Figure 2

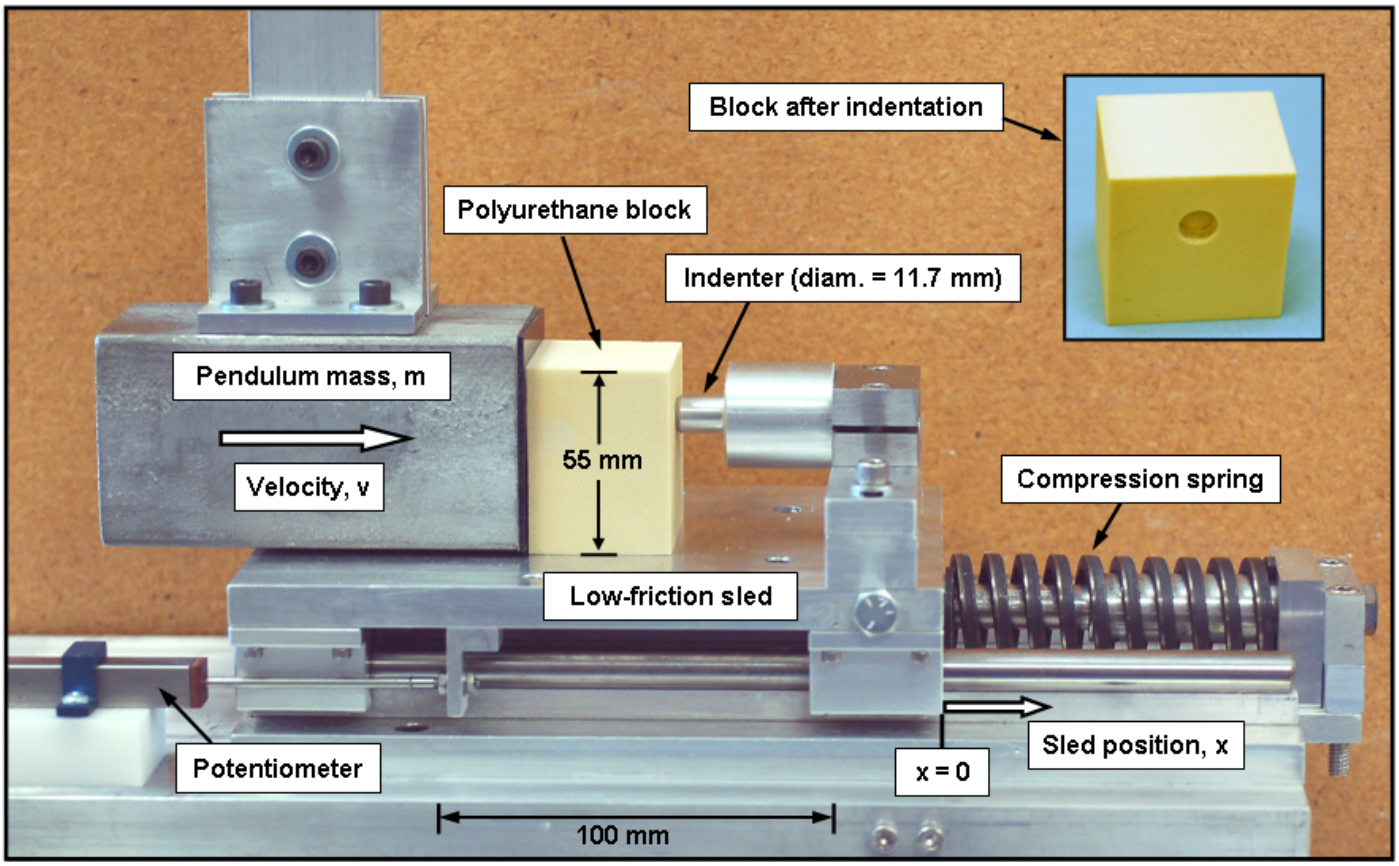
Block after indentation
Polyurethane block
Indenter (diam. = 11.7 mm)
Pendulum mass, m
Velocity, v
55 mm
Compression spring
Low-friction sled
Potentiometer
x = 0
Sled position, x
100 mm

Figure 3

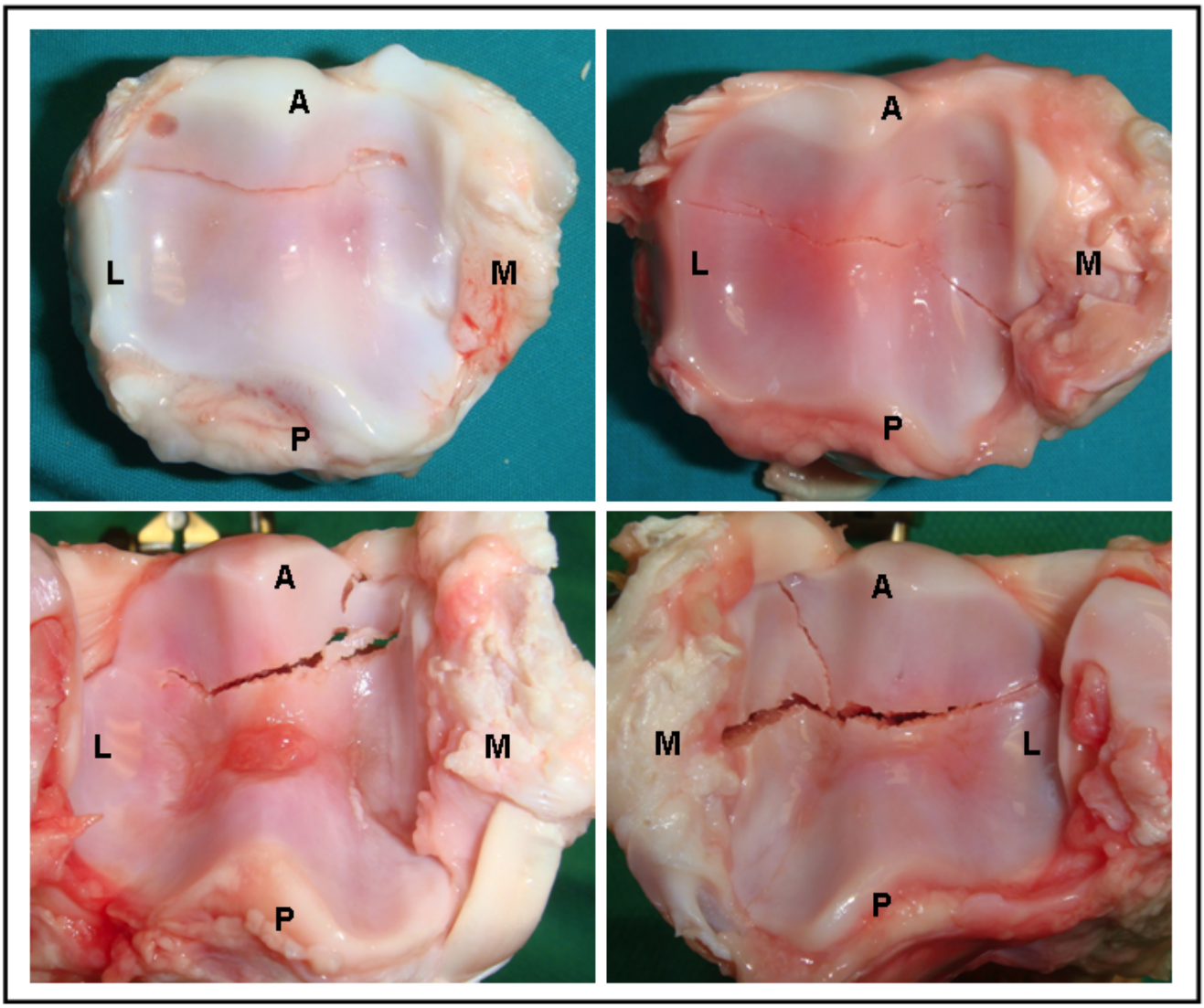

Figure 4

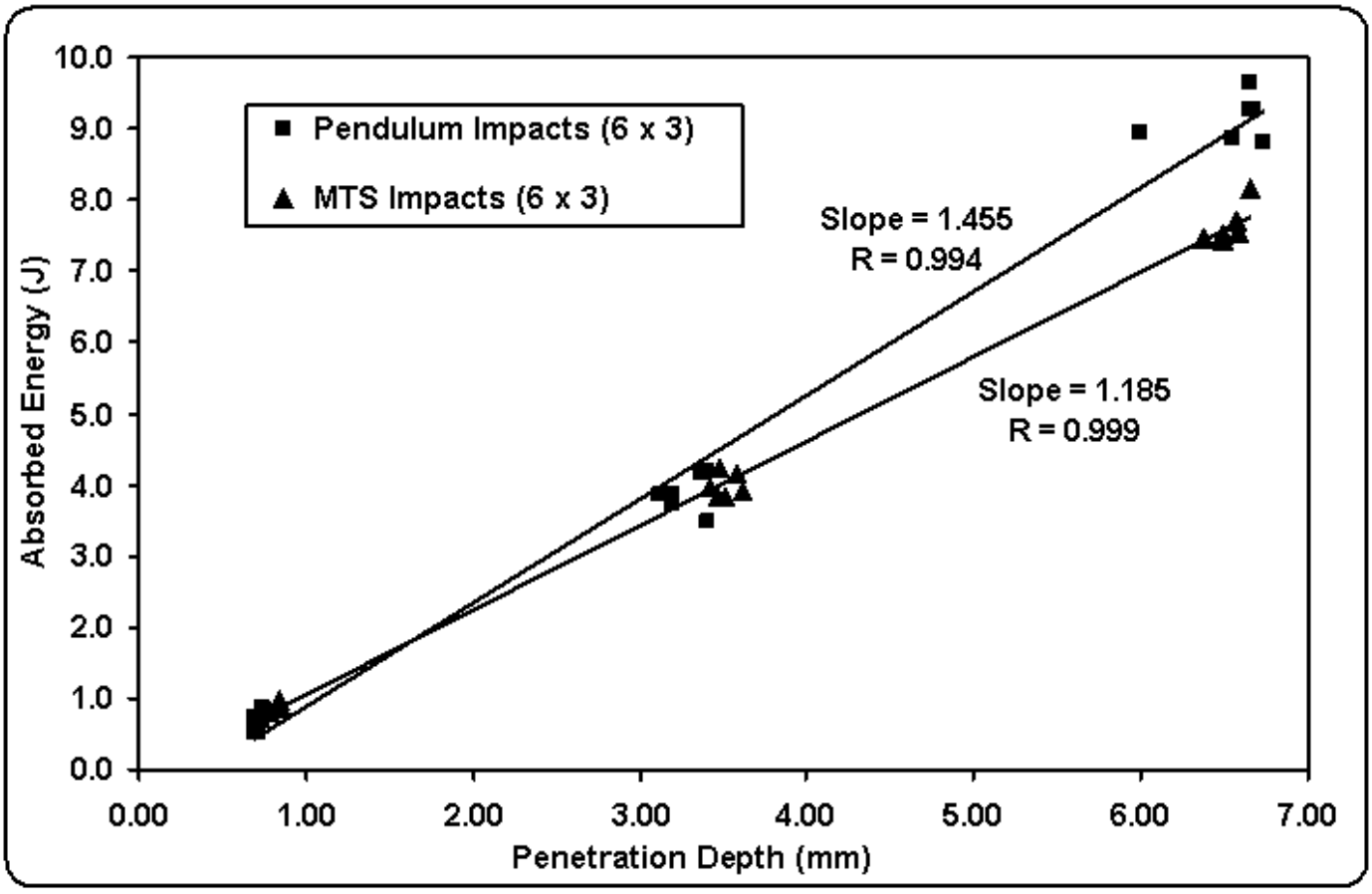
Pendulum Impacts (6 x 3)
MTS Impacts (6 x 3)
Slope = 1.455
R = 0.994
Slope = 1.185
R = 0.999
Absorbed Energy (J)
Penetration Depth (mm)
10.0
9.0
8.0
7.0
6.0
5.0
4.0
3.0
2.0
1.0
0.0
0.00
1.00
2.00
3.00
4.00
5.00
6.00
7.00

Figure 5

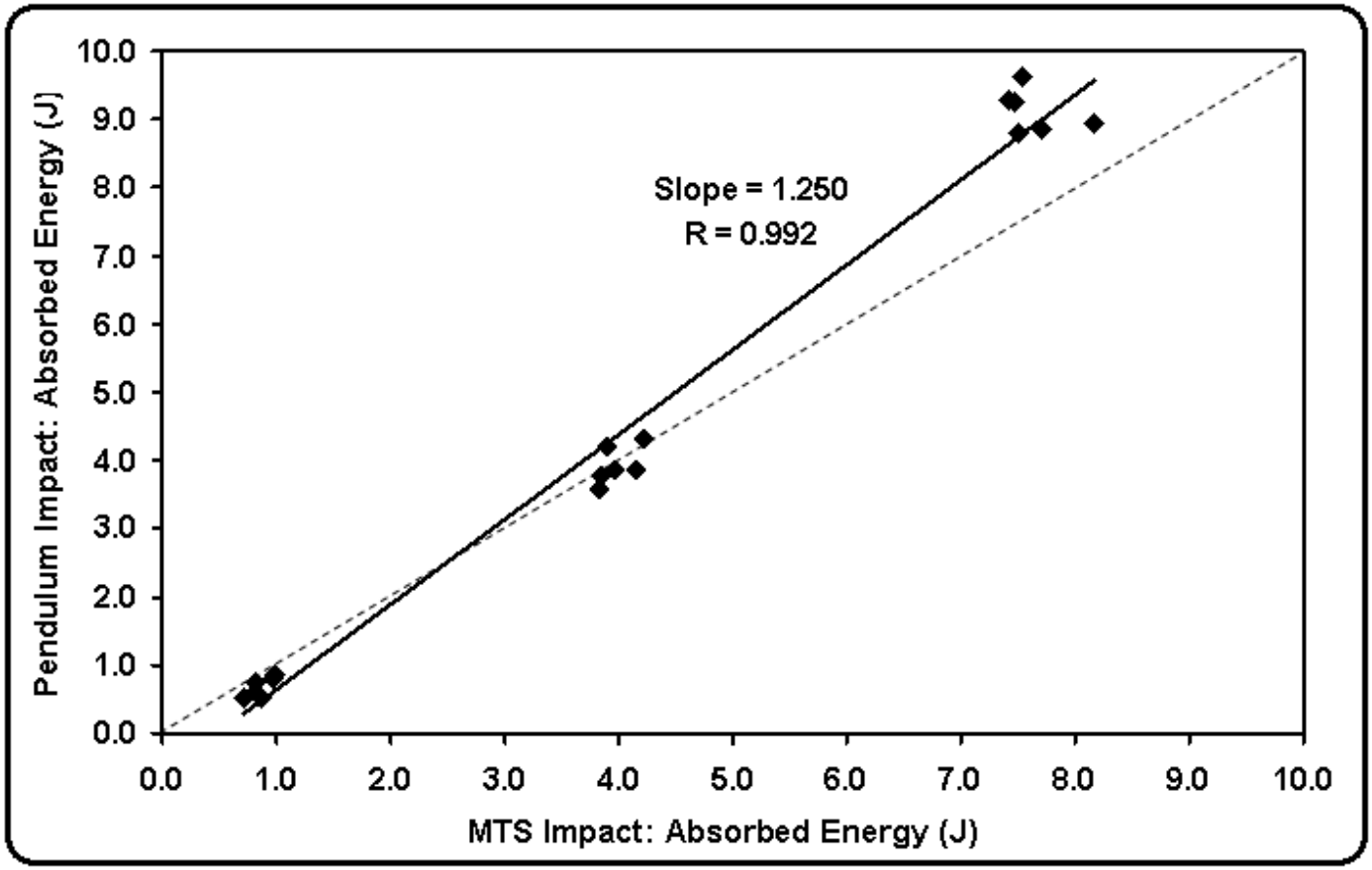
Pendulum Impact: Absorbed Energy (J)
MTS Impact: Absorbed Energy (J)
Slope = 1.250
R = 0.992
0.0
1.0
2.0
3.0
4.0
5.0
6.0
7.0
8.0
9.0
10.0

Figure 6

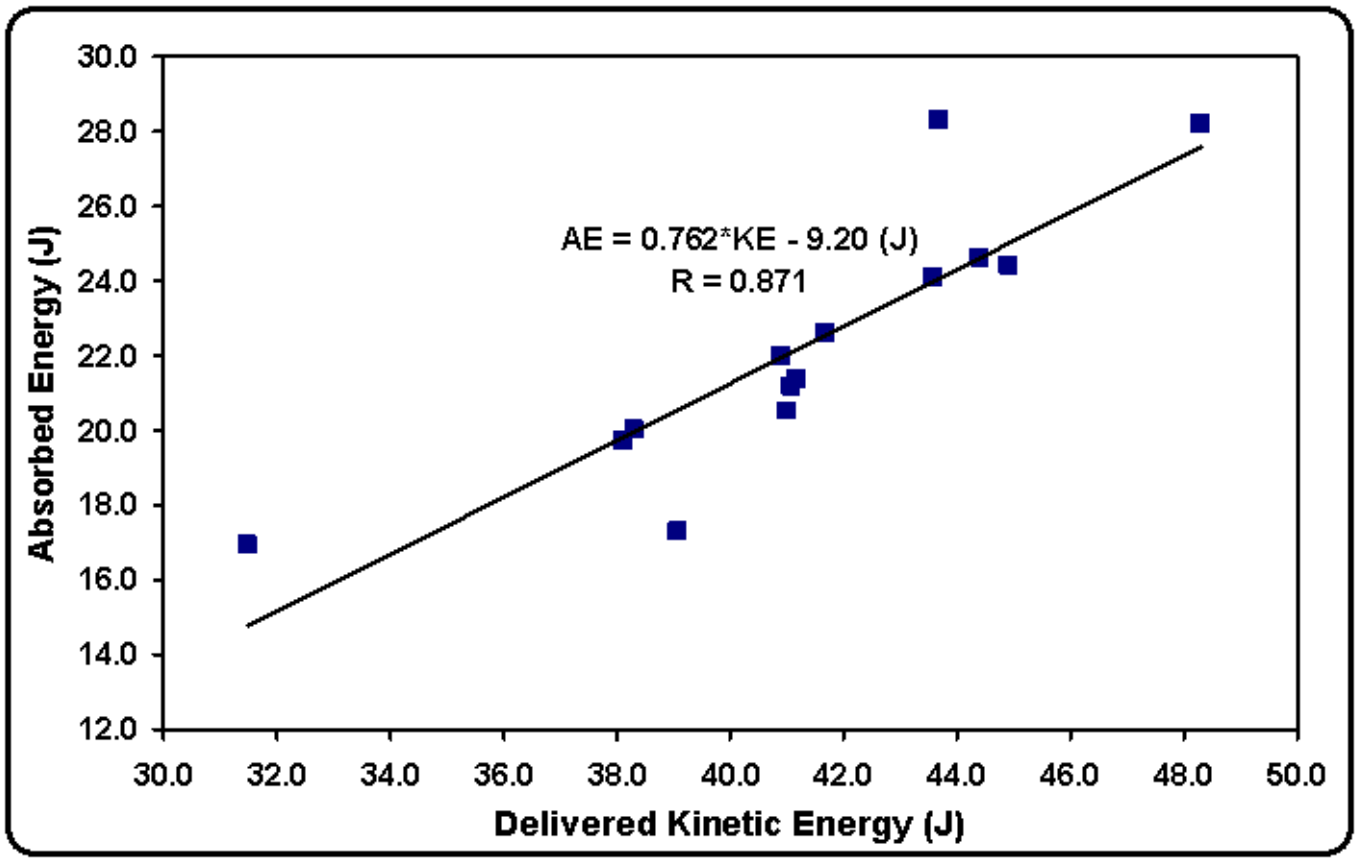
30.0
28.0
26.0
24.0
22.0
20.0
18.0
16.0
14.0
12.0
Absorbed Energy (J)
AE = 0.762*KE - 9.20 (J)
R = 0.871
30.0
32.0
34.0
36.0
38.0
40.0
42.0
44.0
46.0
48.0
50.0
Delivered Kinetic Energy (J)

Table 1

Pendulum-Applied Impacts 3 Drop Heights (n = 6)		MTS-Applied Impacts 3 target penetration depths (n = 6)	
Absorbed Energy Avg. (sd.) (J)	Penetration Depth Avg. (sd.) (mm)	Absorbed Energy Avg. (sd.) (J)	Penetration Depth Avg. (sd.) (mm)
0.80 (0.09)	**0.67** (0.11)	**0.82** (0.08)	**0.74** (0.08)
3.82 (0.11)	**3.29** (0.14)	**4.01** (0.11)	**3.52** (0.11)
9.21 (0.33)	**6.92** (0.17)	**7.63** (0.16)	**6.55** (0.12)

Table 2

Animal #	Kinetic Energy KE (J)	Through-passed Energy TE (J)	Absorbed Energy AE = KE – TE (J)	AE/KE (%)
1	31.5	14.7	16.9	53.5
2	43.7	15.4	28.3	64.7
3	41.2	19.8	21.4	51.9
4	38.1	18.4	19.7	51.6
5	41.1	19.9	21.2	51.6
6	38.3	18.3	20.0	52.2
7	41.7	19.1	22.6	54.2
8	41.0	20.6	20.5	49.9
9	39.1	21.8	17.3	44.2
10	40.9	18.9	22.0	53.9
11	43.6	19.5	24.1	55.2
12	44.9	20.5	24.4	54.4
13	48.3	20.0	28.2	58.4
14	44.4	19.8	24.6	55.3
Average (sd.)	**41.3 (4.0)**	**19.0 (1.9)**	**22.2 (3.5)**	**53.6 (4.5)**

Fluctuations of synovial fluid inflammatory cytokine concentrations in an animal model of intra-articular fracture

Roberts N[1], Martin J[1], Fredericks D[1], Tochigi Y[2], Goetz J[1]

[1]University of Iowa Department of Orthopaedics, [2]Department of Orthopaedics Dokkyo Medical University Koshigaya Hospital

Introduction: Post-traumatic osteoarthritis (OA) is a common outcome subsequent to intra-articular fracture (IAF). It has been hypothesized that the initial inflammatory response to articular injury may be a major factor contributing to OA development. Blocking the initial inflammatory response may help to prevent the development of post-traumatic OA, however investigations of such treatments require pre-clinical investigation in a realistic animal model [1]. The hock of the Yucatan mini-pig is a promising model that allows for the induction of controlled mechanical injuries and treatment with human-like surgical fixation. The mini-pig hock is also large enough to allow for harvest of sufficient volumes of joint fluid and cartilage from which to analyze biological response to injury and potential therapeutic interventions [2]. Dramatic changes in cytokine concentrations have been linked with both acute and chronic inflammation in human osteoarthritis, and the purpose of this work was to determine if similar changes in inflammatory cytokines occur in the synovial fluid of the fractured mini-pig hock.

Methods: Under IACUC approval, an intra-articular fracture was induced in the hock joint (analogous to the human ankle) of 15 Yucatan mini-pigs using a custom-developed pendulum device [2]. The fracture was repaired using a combination of plates and screws, and the leg was casted for one week. Animals were allowed unrestricted pen activity for 12 weeks before sacrifice. Animals were anesthetized and synovial fluid was drawn from both the operated and intact contralateral hock pre-operatively and post-operatively at day 3, and at 1, 2, 4, 8 and 12 weeks. A porcine multiplex cytokine array (Raybiotech, Norcross GA) was used to measure concentrations of ten cytokines (IL1β, IL4, IL6, IL8, IL10, IL12, GMCSF, INFγ, TNF and TGFβ) from the synovial fluid drawn from the fractured and surgically repaired hock and from the non-injured contralateral hock. A one-way analysis of variance with a significance level of 0.05 was performed to compare cytokine concentrations at each post-operative time point with pre-operative values.

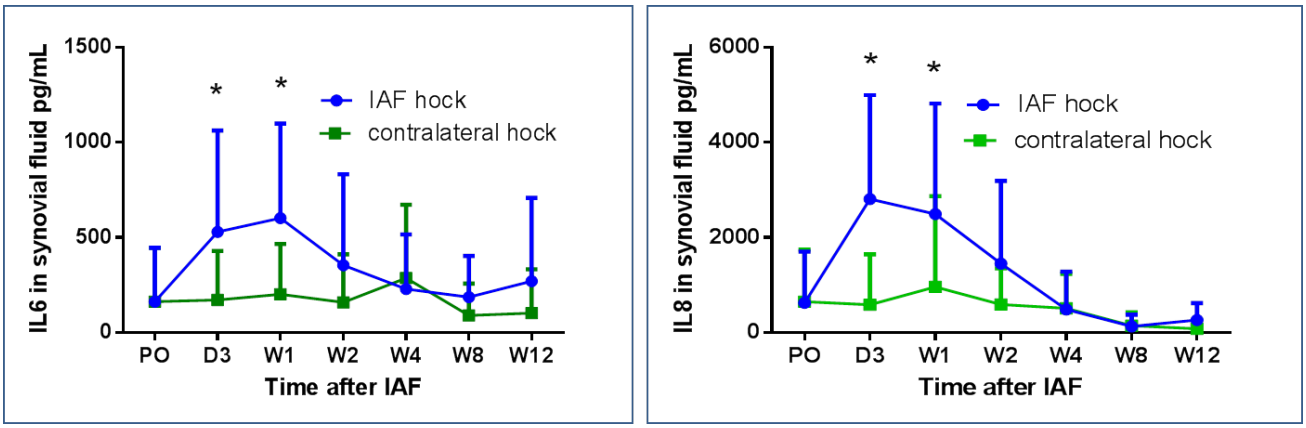

Figure 1: Time-related changes in IL6 and IL8 concentrations in mini-pig hock synovial fluid. PO=pre-IAF, D3=day 3 post-IAF, W1=one week post-IAF, W2= 2 weeks post-IAF, W4= 4 weeks post-IAF, W8= 8 weeks post-IAF, W12= 12 weeks post-IAF, *= significant difference from PO.

Results: Interleukin 6 (IL6) and interleukin 8 (IL8) concentrations increased significantly and conclusively in the injured hock at the Day-3 ($p<0.001$ for IL6 and IL8) and Week-1($p<0.001$ for IL6 and IL8) time points. The concentrations of the other eight cytokines measured were not significantly different from pre-operative values at any post-operative time points. However, these non-significant results were inconclusive, as the power of the tests were well below the desired level of 0.8. Thus, additional data from an increased number of samples could potentially reveal significant differences in cytokine levels that showed trends toward injury-related increases (TGFβ, IL4, GMCSF) or decreases (IL10, INFγ).

Discussion: Lacking precedent synovial fluid cytokine studies in human IAF patients, the inflammatory cytokine response in the fractured mini-pig hock can best be compared to human patients with a torn ACL. In acutely (0-23days) injured human ACL patients, IL6 was elevated a mean of 1600-fold over normal values and IL8 was elevated 7.6-fold over normal values [3]. This trend is similar to the 200-fold increase in IL6 and the 4.5-fold increase in IL8 seen in the mini-pig hock over a similar time period. While the standard deviations in concentrations of all ten cytokines measured in this work were relatively large, the wide range in any given cytokine concentration in mini-pig synovial fluid (e.g. 0 to 6,200 pg/mL for IL8 in injured joints) was in fact narrower than the reported range of cytokine concentrations in human synovial fluid (4.6 to 30,574.8 pg/mL [3]). Because IL6 and IL8 could be ideal prognostic candidates for the development of OA (as both cytokines are involved in initial and chronic inflammation associated with OA), verifying that these cytokines mirror the trends seen in human joint injury was critical for ensuring the relevance of the mini-pig IAF model. In the future, we plan to compare cytokine responses in the mini-pig model with cytokine concentrations measured in synovial fluid from patients with intra-articular ankle fractures to further validate the model.

Significance: Both IL6 and IL8 are present at significantly higher levels in synovial fluids of OA patients [4]. These two cytokines were found to be elevated in the mini-pig hock synovial fluid within the acute phase following an intra-articular fracture. The similarity between the inflammatory response to IAF in the mini-pig and to a joint injury in humans indicates that the mini-pig is a valid model for human-like IAF.

Acknowledgements: This work was funded by Department of Defense grant W81XWH-10-1-0864.

References:

[1]McKinley TO, Borrelli J, D'Lima DD, Furman BD, Giannoudis PV."Basic Science of Intraarticular Fractures and Posttraumatic Osteoarthritis". J Orthop Trauma. 2010 24(9): 567–70.

[2]Di**e**stelmeier BW, Rudert MJ, Tochigi Y, Baer TE, Fredericks DC, Brown TD. "An instrumented pendulum system for measuring energy absorption during fracture insult to large animal joints in vivo." J Biomechanical Engineering 2013

[3]Swärd P, Frobell R, Englund M, Roos H, Struglics A. "Cartilage and bone markers and inflammatory cytokines are increased in synovial fluid in the acute phase of knee injury (hemarthrosis) e a cross-sectional analysis". Osteoarthritis and Cartilage 20 (2012)

[4]Cameron ML, Fu FH, Paessler HH, Schneider M, Evans CH. "Synovial fluid cytokine concentrations as possible prognostic indicators in the ACL-deficient knee". Knee Surg, Sports Traumatol, Arthroscopy (1994) 2:38-44

Intraarticular Administration of N-Acetylcysteine and Glycyrrhizin Alleviates Acute Oxidative Stress Following Intraarticular Fracture

Intraarticular fractures (IAFs) affecting weight bearing have long been associated with poor prognosis and profoundly increased risk of development of post-traumatic osteoarthritis (PTOA) (1). We have recently developed a new model of IAF in which the tibial surface of Yucatan mini-pig hock (ankle) joints is reproducibly fractured without surgical disruption of the capsule (2). In order to demonstrate the utility of this model for future study of potential interventions abrogating PTOA development following IAF, a cocktail of novel pharmaceuticals delivered using a hydrogel vehicle designed for slow drug release was applied to injured joints post-fracture. This cocktail contained 10 mM n-acetylcysteine (NAC), a potent antioxidant, and 100 μM glycyrrhizin (GLZ), an anti-inflammatory agent. This therapy was applied to test the hypothesis that IAF initiates acute oxidative stress in conjunction with increased inflammation in the injured joint, contributing to cellular damage and dysfunction associated with PTOA development.

Though contributory to numerous disease states, oxidative stress following intraarticular fracture has not been directly assessed *in vivo* following IAF. However, following intraarticular fracture, given the flood of oxygen and blood into the joint, a physiological setting normally relatively devoid of both, it is logical to suppose that oxidative stress may be occurring and deleteriously impacting chondrocyte function. Specifically, this may proceed similarly to well-characterized ischemia/reperfusion phenomena in a cardiovascular setting, in which the addition of NAC has shown some efficacy in reducing oxidation occurring as a result of overproduction of reactive oxygen species (ROS) in the presence of excess oxygen and iron (3). NAC operates by freely crossing cellular membranes into the cytosol where it is rapidly deacetylated to form cysteine. This additional cysteine is capable of operating as an antioxidant on its own (most famously detoxifying acetaminophen in cases of accidental overdose) but also acts as a supplement to glutathione (GSH) production by the cell (4). GSH is a tripeptide thiol that acts as the primary redox buffer of the cell, contributing to maintenance of the overall reduced environment of the cell with a concentration in the millimolar range in most mammalian cells. Oxidation of GSH to glutathione disulfide (GSSG) is rapidly reversible under normal conditions, but requires the consumption of NADPH. Therefore, in cases where a cell is truly under oxidative stress, as opposed to simply oxidatively damaged, GSSG will slowly begin to accumulate and the GSH-GSSG couple with appear more oxidized, i.e. %GSSG or GSSG/total GSH will increase. This is viewed as a standard measure of oxidative stress as distinct from oxidative damage.

In order to test for the presence of oxidative stress following IAF, anesthetized pigs were subjected to a 45 J impact to the distal tibia, producing observable IAFs which were then anatomically reduced and surgically plated. All surgeries were conducted under IACUC approved protocols. Either 0.5 mL hydrogel vehicle or 0.5 mL hydrogel containing 10 mM NAC and 100 μM GLZ was injected directly into the joint immediately post operatively and again 24 hours later. Normal pigs receiving no surgery served as negative controls and inflammation-positive pigs receiving an identical IAF followed by hydrogel containing endotoxin served as positive controls. All operated pigs (n=3 to date) were casted for one week, at the end of which the animal was sacrificed and cartilage was fresh harvested from the articular surface, homogenized in 5% sulfosalicylic acid to protect against GSH autoxidation, and analyzed for GSH/GSSG content according to the GSH reductase-recycling method of OW Griffith (5). Data were determined as fold difference in %GSSG (of total GSH) between hocks enduring fractures (left) and the corresponding contralateral, healthy hocks (right). A small piece of articular cartilage from each hock was also digested and harvested chondrocytes were plated for analysis on the Seahorse XF-96 Extracellular Flux Analyzer. This sophisticated instrument is capable of querying the mitochondrial health of living cells on a per cell basis. By measuring oxygen consumption in the presence of a partial and total respiratory blockade, the number of protons displaced and subsequently relaxing back across the mitochondrial membrane without generating ATP, so-called proton leakage, can be determined. This quantity is indicative of the health of the mitochondrial membrane, often an early target of oxidative stress.

Data from both hydrogel IAF hocks and positive control IAF hocks demonstrated increased oxidation of the GSH-GSSG couple relative to contralateral hocks from the same animal (Figure 1). This oxidation was ameliorated with addition of 10 mM NAC and 100 μM GLZ immediately post-fracture, returning GSSG levels to those of normal, uninjured pigs. Hydrogel IAF hocks also demonstrated an increased amount of proton leakage relative to contralateral hocks which is not present in those hocks receiving NAC/GLZ, further supporting the hypothesis that NAC/GLZ is capable of preventing cellular oxidative stress (Figure 2). These data suggest that NAC/GLZ injections are interrupting joint pathology contributing to the commencement of oxidative stress following IAF. Given recent findings concerning the mitochondrial and redox disruptions present in osteoarthritic chondrocytes, data presented here represent a promising step towards potential antioxidant, anti-inflammatory interventions targeted at preventing oxidative stress with the intention of slowing PTOA progression. We have not yet determined the specific roles of the antioxidant NAC and the anti-inflammatory GLZ. Further, the impact of these findings upon joint health and early indications of PTOA has not yet been evaluated; however, these data demonstrate that the porcine hock IAF model is capable of distinguishing physiological, biochemical differences among treatment groups following IAF. We believe our data indicate that the Yucatan mini-pig model of IAF can be applied as a powerful tool for advanced testing of pharmaceutical approaches to preventing PTOA after IAF.

Funding for this work was provided by the Department of Defense grant #W81XWH-10-1-0864.

1. Tylman et al. Clin Orthop Relat Res. 1991; 272.; 2. Diestelmeier et al. J Biomechanical Engineering 2013 (Accepted).; 3. Ceconi et al. J Mol Cell Cardiol. 1988; 20(1).; 4. De Flora et al. Carcinogenesis 1985; 6(12).; 5. Griffith. Anal Biochem 1980; 106(1).

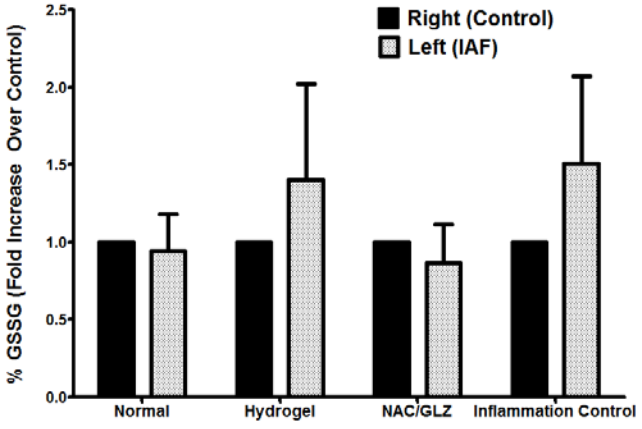

Figure 1. N-Acetylcysteine (NAC) and Glycyrrhizin (GLZ) Injection Prevent Oxidation of the Glutathione Redox Couple Following Intraarticular Fracture (IAF)

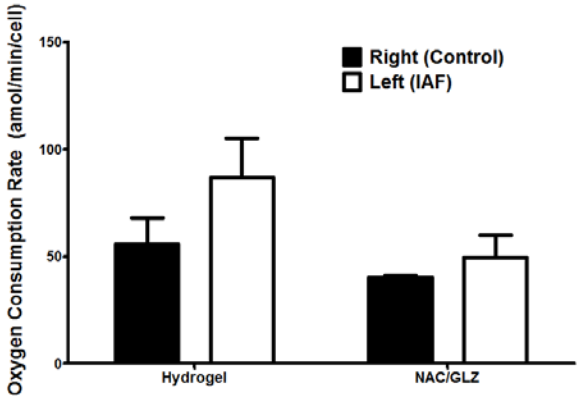

Figure 2. N-Acetylcysteine (NAC) and Glycyrrhizin (GLZ) Injection Prevent Increases in Mitochondrial Proton Leakage Associated with Intraarticular Fracture